Molecular Plant Pathology

MOLECULAR PLANT PATHOLOGY (2018) 19(5), 1222–1237 DOI: 10.1111/mpp.12612

Hijacking of the nucleolar protein fibrillarin by TGB1 is required for cell-to-cell movement of *Barley stripe mosaic virus*

ZHENGGANG LI, YONGLIANG ZHANG, ZHIHAO JIANG, XUEJIAO JIN, KUN ZHANG, XIANBING WANG, CHENGGUI HAN, JIALIN YU AND DAWEI LI *

State Key Laboratory of Agro-Biotechnology and Ministry of Agriculture Key Laboratory of Soil Microbiology, College of Biological Sciences, China Agricultural University, Beijing 100193, China

SUMMARY

Barley stripe mosaic virus (BSMV) Triple Gene Block1 (TGB1) is a multifunctional movement protein with RNA-binding, ATPase and helicase activities which mainly localizes to the plasmodesmata (PD) in infected cells. Here, we show that TGB1 localizes to the nucleus and the nucleolus, as well as the cytoplasm, and that TGB1 nuclear-cytoplasmic trafficking is required for BSMV cell-to-cell movement. Prediction analyses and laser scanning confocal microscopy (LSCM) experiments verified that TGB1 possesses a nucleolar localization signal (NoLS) (amino acids 95–104) and a nuclear localization signal (NLS) (amino acids 227–238). NoLS mutations reduced BSMV cell-to-cell movement significantly, whereas NLS mutations almost completely abolished movement. Furthermore, neither the NoLS nor NLS mutant viruses could infect *Nicotiana benthamiana* systemically, although the NoLS mutant virus was able to establish systemic infections of barley. Protein interaction experiments demonstrated that TGB1 interacts directly with the glycine–arginine-rich (GAR) domain of the nucleolar protein fibrillarin (Fib2). Moreover, in BSMV-infected cells, Fib2 accumulation increased by about 60%–70% and co-localized with TGB1 in the plasmodesmata. In addition, BSMV cell-to-cell movement in *fib2* knockdown transgenic plants was reduced to less than one-third of that of non-transgenic plants. Fib2 also co-localized with both TGB1 and BSMV RNA, which are the main components of the ribonucleoprotein (RNP) movement complex. Collectively, these results show that TGB1–Fib2 interactions play a direct role in cell-to-cell movement, and we propose that Fib2 is hijacked by BSMV TGB1 to form a BSMV RNP which functions in cell-to-cell movement.

Keywords: *Barley stripe mosaic virus*, cell-to-cell movement, fibrillarin (Fib2), nuclear localization, nucleolus, TGB1.

INTRODUCTION

The nucleus is a membrane-enclosed organelle containing the nucleolus, Cajal bodies, promyelocytic leukaemia bodies, splicing speckles, paraspeckles and other subnuclear bodies (Dundr & Misteli, 2001; Matera *et al.*, 2009). The nucleolus is the most prominent subnuclear compartment in which rRNA transcription, processing and ribosomal subunit assembly occur (Boisvert *et al.*, 2007; Dubois & Boisvert, 2016). Fibrillarin (Fib2), nucleolin and B23 are the most abundant and well-studied nucleolar proteins (Dubois & Boisvert, 2016).

A growing body of evidence has suggested that the nucleolus is involved in the infection, replication and movement of a number of viruses (Hiscox, 2007; Rawlinson & Moseley, 2015; Taliansky *et al.*, 2010), and that virus-encoded proteins may traffic into the nucleolus to alter the nuclear structure, or to redistribute nucleolar proteins involved in replication and movement (Rawlinson & Moseley, 2015; Taliansky *et al.*, 2010). For example, protein V, encoded by the double-stranded DNA (dsDNA)-containing Adenovirus, associates with nucleoli, where it functions to relocate nucleolin and the B23 protein from the nucleolus to the cytoplasm (Matthews, 2001). Adenovirus-associated virus (AAV) utilizes B23 to mediate the formation of the Cap and Rep complexes (Bevington *et al.*, 2007). Some RNA viruses also encode one or more proteins that traffic into the nucleolus and result in the disruption of nucleolar architecture and function (Greco, 2009; Hiscox, 2007). Previous studies have shown that poliovirus inactivates the RNA polymerase I upstream binding factor in infected cells to inhibit rRNA transcription (Banerjee *et al.*, 2005). The poliovirus 3′ non-coding region also interacts with nucleolin and results in selective redistribution to the cytoplasm (Waggoner & Sarnow, 1998). In the cytoplasm, nucleolin stimulates internal ribosome entry site (IRES)-dependent translation by direct binding to IRESs in the poliovirus 5′ untranslated region (Hellen & Sarnow, 2001).

In a plant potyvirus, *Potato virus A* (PVA), two regions of the genome-linked protein (VPg) domain, designated NLS-I and NLS-II, contain nuclear (NLS) and nucleolar (NoLS) localization signals, and interact with Fib2, whose depletion reduces virus accumulation (Rajamaki & Valkonen, 2009). The nuclear inclusion protein a (NIa) also associates with infected cell nuclei (Rajamaki & Valkonen, 2009). A separate study has shown that the P20 protein encoded by *Bamboo mosaic virus* (BaMV) satRNA (satBaMV) co-localizes with Fib2 in the nuclei, and that down-regulation of Fib2 inhibits the long-distance movement of satBaMV, but not BaMV (Chang *et al.*, 2016). Moreover, *Rice stripe virus* (RSV) p2 also interacts with Fib2, and Fib2 depletion abolishes long-distance

* *Correspondence*: Email: Dawei.Li@cau.edu.cn

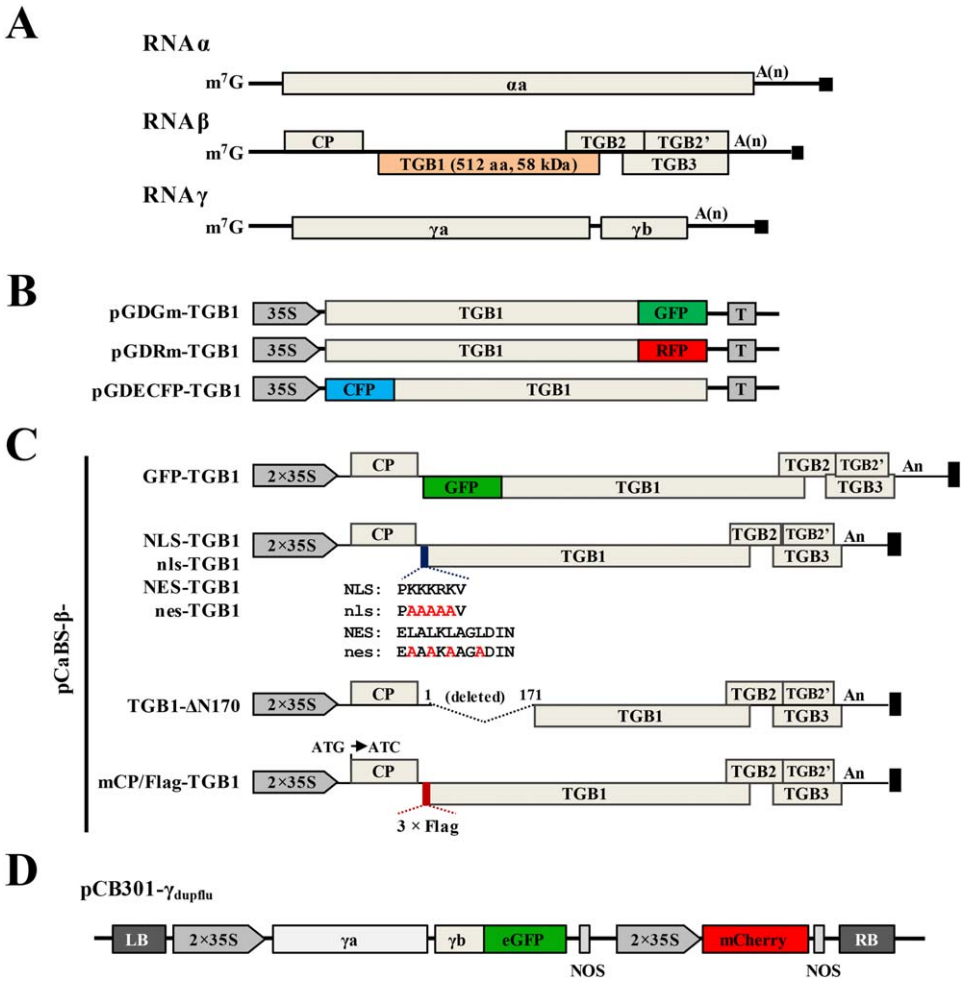

Fig. 1 *Barley stripe mosaic virus* (BSMV) genome organization and mutant Triple Gene Block1 (TGB1) constructs used in the experiments. (A) Schematic diagram of the BSMV genomic RNAs. CP, coat protein. (B) Green, red and cyan fluorescent protein (GFP, RFP and CFP) TGB1 reporter constructs used for subcellular localization. (C) Infectious RNAβ clones used in this study. (D) Structure of the pCB301-γ_{dupflu} cassette used to discriminate between primary infection foci and BSMV cell-to-cell movement. The cassette was inserted between left border (LB) and right border (RB) regions of pCB301-2 × 35S-MCS-HDV_{Rz}-NOS (Yao *et al.*, 2011).

RSV movement (Zheng *et al.*, 2015). In another example, the umbravirus, *Groundnut rosette virus* (GRV), the movement protein (MP) ORF3 enters into the nucleolus to recruit Fib2 to infectious ribonucleoproteins (RNPs) in the cytoplasm (Canetta *et al.*, 2008; Kim *et al.*, 2007a,b). *Beet black scorch virus* (BBSV) p7a also localizes to the nucleolus and interacts with Fib2 (Wang *et al.*, 2012). In addition, the Triple Gene Block1 (TGB1) proteins of *Potato mop-top virus* (PMTV) and *Poa semilatent virus* (PSLV) also co-localize with Fib2 in the nucleolus, but the effects of these interactions on infectious processes are unknown (Lukhovitskaya *et al.*, 2015; Semashko *et al.*, 2012).

Barley stripe mosaic virus (BSMV) is the type member of the genus *Hordeivirus* which contains three segmented genomic RNAs (gRNAs) designated α, β and γ (Fig. 1A) (Bragg *et al.*, 2008). RNAα encodes the αa protein subunit of the RNA-dependent RNA polymerase (RdRp) complex. RNAβ serves as the mRNA for the coat protein (CP), which is dispensable for cell-to-cell and long-distance movement, and three major MPs (TGB1, TGB2 and TGB3) that are expressed from subgenomic RNAβ1 (sgRNAβ1) and sgRNAβ2, respectively. RNAγ encodes the polymerase subunit γa of the RdRp complex, and the multifunctional γb protein, which functions as a viral suppressor of RNA silencing (VRS) (Bragg & Jackson, 2004; Yelina *et al.*, 2002), a modulator of host defences (Jackson *et al.*, 2009) and an enhancer of αa helicase activity (Zhang *et al.*, 2017). BSMV TGB1 is a multifunctional protein with ATPase, RNA-binding and RNA helicase activities (Donald *et al.*, 1997; Kalinina *et al.*, 2002; Verchot-Lubicz *et al.*, 2010). The C-terminus of TGB1 contains seven conserved motifs associated with helicase and RNA-binding activities (Lawrence & Jackson, 2001b; Lim *et al.*, 2008; Morozov & Solovyev, 2003), and binds BSMV gRNAs and sgRNAs to form RNP complexes that are thought to be involved in cell-to-cell movement (Lim *et al.*, 2008). Direct binding of TGB3 by TGB1 and indirect interactions with TGB2 are also required for spread to adjacent cells (Jackson *et al.*, 2009; Lawrence & Jackson, 2001b; Lim *et al.*, 2008). TGB1 localizes primarily to the cytoplasm when expressed alone, and mainly to the cell wall during infection and in the presence of TGB3 (Lawrence & Jackson, 2001a; Lim *et al.*, 2009). Optimal cell wall localization of TGB1 requires interactions between TGB2 and TGB3 at a ratio of ~100 : 10 : 1 (Lim *et al.*, 2009). TGB1 self-interactions

are not required for TGB1 cell wall localization, but mutation of the helicase motifs results in the redistribution of TGB1 from the cell wall to the cytoplasm (Jackson *et al.*, 2009; Lawrence & Jackson, 2001a; Lim *et al.*, 2008, 2009). Phosphorylation of TGB1 by the host protein kinase CK2 at Thr401 is also critical for BSMV movement in monocots and dicots (Hu *et al.*, 2015). In addition to its biochemical properties and roles in movement, TGB1 also serves as an avirulence determinant to elicit resistance against several BSMV strains in *Brachypodium distachyon* inbred lines containing the *Bsr1* resistant gene (Cui *et al.*, 2012; Lee *et al.*, 2012).

Here, we show that BSMV TGB1 partially localizes to the nucleus and the nucleolus when expressed alone, or in BSMV-infected cells. We also find that TGB1 nuclear-cytoplasmic trafficking is required for BSMV cell-to-cell and long-distance movement, and also interacts with the main nucleolar protein, Fib2. Downregulation of *fib2* reduces BSMV cell-to-cell movement and accumulation in inoculated leaves, and Fib2 co-localizes with BSMV viral RNA (vRNA) near the cell wall. Taken together, our results support a model whereby Fib2 is hijacked by TGB1 to form a Fib2–RNP movement complex that is required for BSMV cell-to-cell movement.

RESULTS

Nuclear-cytoplasmic trafficking of TGB1 is required for BSMV infection

BSMV TGB1 localizes primarily to the cell wall in BSMV-infected cells or when co-expressed with TGB2 and TGB3 at a ratio of ~100 : 10 : 1 (Lawrence & Jackson, 2001a; Lim *et al.*, 2009). A recent study from our laboratory has reported that a portion of TGB1 is distributed in both the cytoplasm and nuclei of *Nicotiana benthamiana* leaf cells during co-expression with TGB1 and protein kinase CK2α proteins (Hu *et al.*, 2015). To determine more details about the nuclear localization of TGB1, green fluorescent protein (GFP)-TGB1 (Lim *et al.*, 2009) was transiently expressed in H2B-red fluorescent protein (RFP) transgenic *N. benthamiana* leaves (Martin *et al.*, 2009) by agroinfiltration and examined by laser scanning confocal microscopy (LSCM) at 3 days post-infiltration (dpi). Under these conditions, confocal microscopy revealed that a considerable amount of GFP-TGB1 was present in both the nuclei and the nucleolus (Fig. 2A, top panel). We also constructed a TGB1-GFP reporter gene (Fig. 1B) with TGB1-specific primers (Table S1, see Supporting Information) and examined the subcellular localization of the protein. Complementary experiments verified that GFP fused to the C-terminus of TGB1 does not affect TGB1 function (data not shown). Consistent with GFP-TGB1 experiments, TGB1-GFP also exhibited both cytoplasmic and nuclear accumulation (Fig. 2A, middle panel). However, unlike the bright punctate foci formed by GFP-TGB1 (Lim *et al.*,

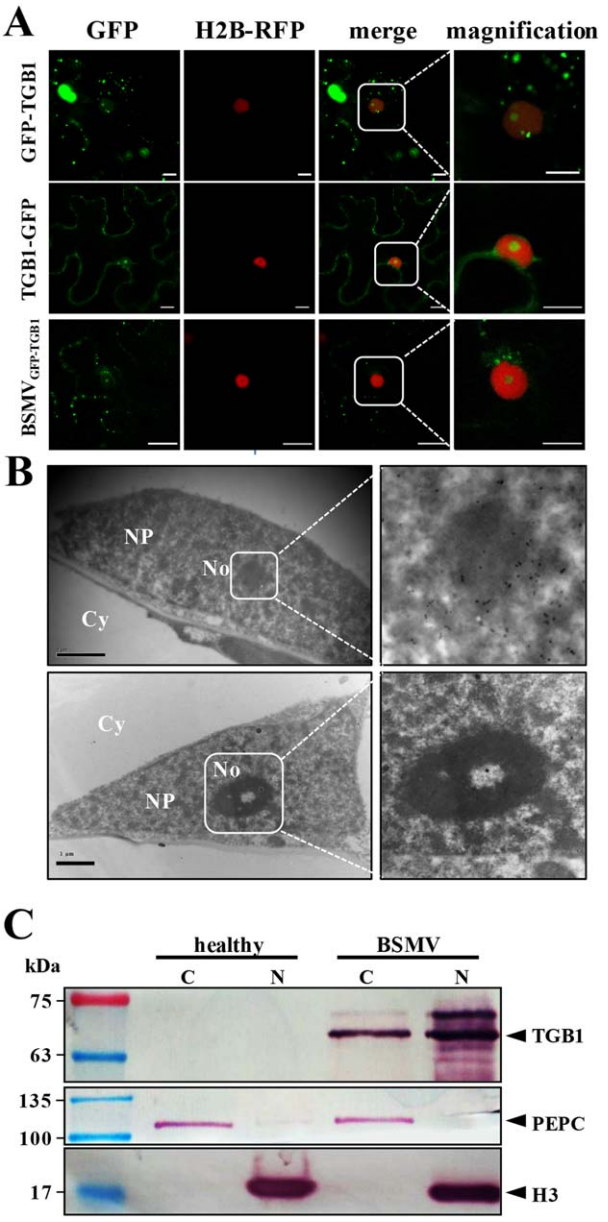

Fig. 2 Triple Gene Block1 (TGB1) nuclear localization when expressed alone or in *Barley stripe mosaic virus* (BSMV)-infected cells. (A) Subcellular localization of transiently expressed GFP-TGB1 (Lim *et al.*, 2009) and TGB1-GFP from agroinfiltrated H2B-RFP transgenic *Nicotiana benthamiana* leaves at 3 days post-infiltration (dpi) or GFP-TGB1 (Fig. 1C) expressed in BSMV-infected leaves. Bars, 10 μm. (B) The top panel shows immunogold detection of TGB1 in the nucleoli of BSMV-infected cells with antibodies specific to TGB1. The bottom panel shows negative control without primary antibody incubation. Cy, cytoplasm; No, nucleolus; NP, nucleoplasm. Bars, 1 μm. (C) Proteins isolated from the cytoplasmic (C) or nuclear (N) fractions of healthy and BSMV-infected leaves. TGB1 is present in both the cytoplasm and the nuclei. Phosphoenolpyruvate carboxylase (PEPC) and histone H3 were used as cytoplasmic and nuclear markers, respectively.

2009) (Fig. 2A, top panel), TGB1-GFP was distributed relatively uniformly throughout the cytoplasm (Fig. 2A, middle panel).

Next, to examine the nuclear localization of TGB1 during infection, we investigated the localization of GFP-TGB1 when expressed from BSMV sgRNAβ1 (Fig. 1C). Consistent with previous reports, in which TGB1 mainly formed intense punctate foci along the cell wall and perinuclear membranes (Lawrence & Jackson, 2001a), a small portion of TGB1 also localized to the nucleus and nucleolus (Fig. 2A, bottom panel). To further verify the nuclear and nucleolar localization of TGB1, immunogold labelling experiments with a TGB1-specific antibody after fixation of BSMV-infected *N. benthamiana* leaves revealed gold particles in the nuclei and nucleoli (Fig. 2B), but particles were not detected in samples without primary antibody incubation (Fig. 2B, bottom panel). In addition, TGB1 was detected in both the cytoplasm and the nuclear fractions in a nuclear isolation experiment (Fig. 2C).

Most nuclear proteins are transported to the nucleus via the well-characterized importin α/β pathway, which depends on the binding of importin α to cargo proteins (Goldfarb *et al.*, 2004; Lange *et al.*, 2007). To identify the nuclear transport pathway responsible for TGB1 targeting, bimolecular fluorescence complementation (BiFC) and glutathione *S*-transferase (GST) pull-down assays were performed to test interactions between TGB1 and importin α. The BiFC experiments showed that cells co-expressing either TGB1-nYFP/Impα-cYFP or TGB1-cYFP/Impα-nYFP (Zhang *et al.*, 2011) reconstituted yellow fluorescent protein (YFP) fluorescence in the nucleus (Fig. S1A, see Supporting Information). Moreover, GST-Impα and TGB1-His protein were also purified from *Escherichia coli* for GST pull-down assays. These experiments demonstrated the binding of TGB1-His and GST-Impα, but the negative GST-GFP control failed to interact with TGB1-His (Fig. S1B). These results suggest that TGB1 nuclear transport may rely on the importin α/β pathway.

To test whether TGB1 nuclear and nucleolar localization is required for infection, TGB1 in RNAβ was fused to several nuclear import or export derivatives (Slootweg *et al.*, 2010). These fusions included the well-known NLS (PKKKRKV) from the SV40 large T-antigen (Kalderon *et al.*, 1984; Lanford & Butel, 1984) and its non-functional nls mutant (PAAAAAV), the nuclear export signal (NES) (ELALKLAGLDIN) from the cyclic adenosine monophosphate (cAMP)-dependent protein kinase inhibitor (PKI) protein (Wen *et al.*, 1995) and its non-functional nes mutant (EAAAKAAGADIN) (Fig. 1C). The subcellular localizations of the NLS, nls, NES and nes fused TGB1-GFP derivatives were evaluated by confocal microscopy of leaf regions expressing the TGB1 derivatives. At 3 days after agroinfiltration, most of the NLS-TGB1 fluorescence originated from the nucleolus, and NES-TGB1 fluorescence was difficult to detect in the nucleus, but the localization of nls-TGB1 and nes-TGB1 was not altered compared with TGB1 (Fig. S2, see Supporting Information). After 5 days, the inoculated leaves were harvested and extracts were subjected to western blot analysis. Although $BSMV_{NLS\text{-}TGB1}$ exhibited much lower abundance than $BSMV_{nls\text{-}TGB1}$ and $BSMV_{nes\text{-}TGB1}$, the latter derivatives both elicited milder symptoms than BSMV. In contrast, $BSMV_{NES\text{-}TGB1}$ accumulation was comparable with BSMV (Fig. 3A).

To further investigate the effects of TGB1 nuclear-cytoplasmic trafficking on BSMV cell-to-cell movement, we developed a BSMV duplex fluorescence system. In this system, an mCherry expression cassette was inserted adjacent to the mini binary vector pCB301-$\gamma_{\gamma b\text{-}GFP}$ to produce pCB301-γ_{dupflu} (Fig. 1D). With this duplex vector, γb-GFP encoded by sgRNAγ emits green fluorescence continuously throughout replication and cell-to-cell movement, whereas mCherry is only expressed in the primary infiltrated cells. Thus, the merged regions with dual fluorescence represent primary infection foci, and the GFP regions lacking mCherry are secondary cells invaded by the BSMV reporter (designated dfBSMV). Consistent with the western blot assays, NLS-TGB1 reduced viral cell-to-cell movement of dfBSMV significantly in *N. benthamiana* at 3 dpi, whereas NES-TGB1 did not significantly affect intercellular movement compared with wild-type (WT), nls-TGB1 and nes-TGB1 (Fig. 3B,C). The cell-to-cell movement of the $dfBSMV_{NLS\text{-}TGB1}$ virus was less than one-third of that of dfBSMV, but the movement of the other dfBSMV mutants was not obviously affected (Fig. 3B,C).

In addition to the cytological effects of the TGB1 mutants, systemic movement of the BSMV derivatives was also examined. In *N. benthamiana* plants infected by $BSMV_{WT}$, $BSMV_{nls\text{-}TGB1}$ and $BSMV_{nes\text{-}TGB1}$ viruses, the upper leaves developed mosaic symptoms by 16 dpi, but the $BSMV_{NLS\text{-}TGB1}$ and $BSMV_{NES\text{-}TGB1}$ mutants failed to develop symptoms after infiltration (Fig. 3D). In addition, enzyme-linked immunosorbent assay (ELISA) (Fig. 3E), reverse transcription-polymerase chain reaction (RT-PCR) (Fig. S3A, see Supporting Information) and systemic infectivity statistics (Table S2, see Supporting Information) further verified that the $BSMV_{NLS\text{-}TGB1}$ and $BSMV_{NES\text{-}TGB1}$ mutants were unable to infect *N. benthamiana* systemically. Taken together, these results demonstrate that, when TGB1 is retained in the nucleus, both local and systemic movement of BSMV are disrupted. However, localized transit from infection foci was evident and systemic infections were abolished when TGB1 was depleted from the nucleus. Hence, nuclear-cytoplasmic trafficking of TGB1 is required for both cell-to-cell and systemic movement of BSMV in *N. benthamiana*.

Both nuclear and nucleolar TGB1 localization signals are required for BSMV movement in *N. benthamiana* and barley

Proteins localized to the nucleus often possess NLSs containing one or more arginine- and lysine-rich motifs. Prediction of NLS signals (Kosugi *et al.*, 2009) revealed that TGB1 contains two NLSs,

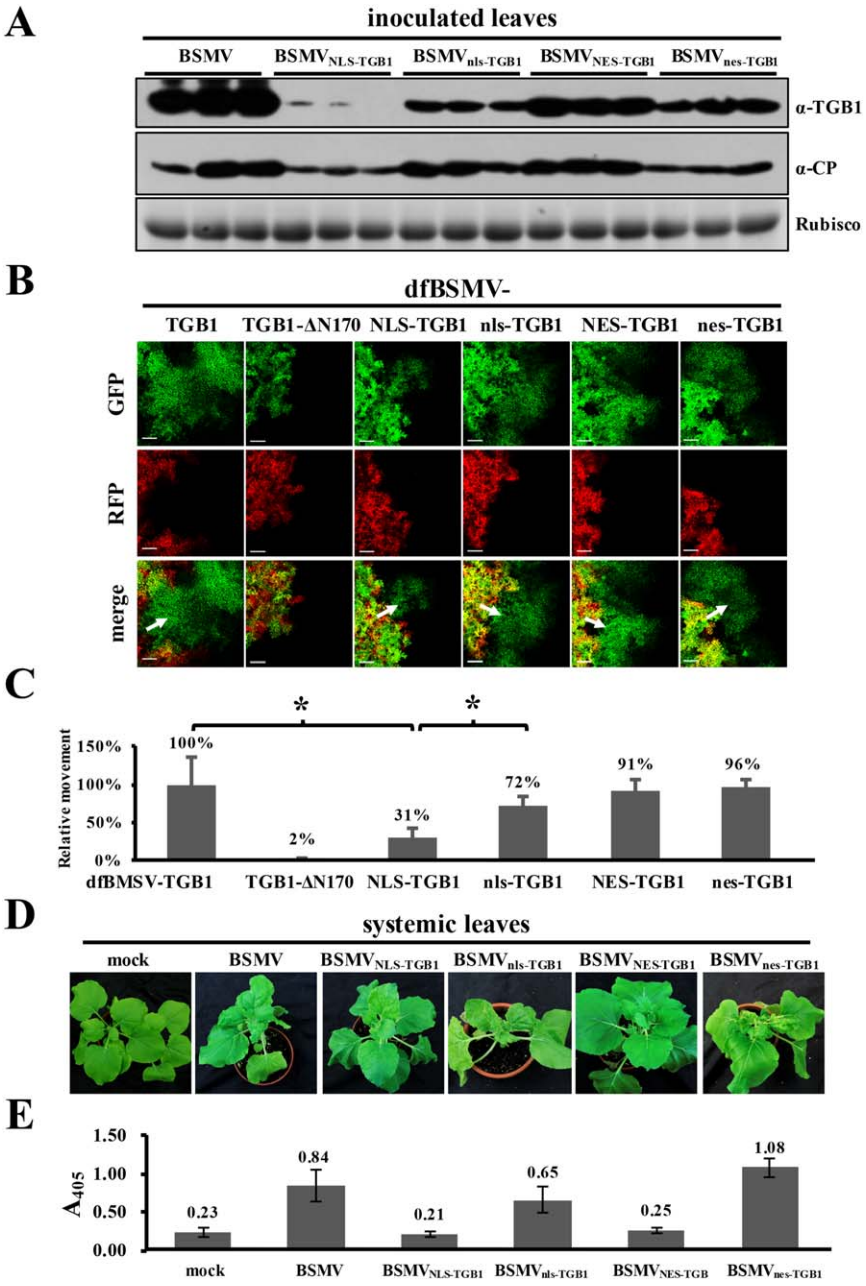

Fig. 3 Effects of Triple Gene Block1 (TGB1) nuclear-cytoplasmic trafficking disruption on *Barley stripe mosaic virus* (BSMV) cell-to-cell and long-distance movement. (A) Western blots showing the accumulation of BSMV and BSMV mutants containing NLS/nls or NES/nes motifs fused to the N-terminus of TGB1 (see Fig. 1C for illustrations of the TGB1 mutants). *Agrobacterium* strains containing RNA α, γ and β, or the β NLS/nls or NES/nes motif mutants, were co-infiltrated into *Nicotiana benthamiana* leaves, and infiltrated leaf samples were extracted at 5 days post-infiltration (dpi). Ribulose-1,5-bisphosphate carboxylase/oxygenase (Rubisco) levels indicate equal sample loading. (B) Cell-to-cell movement of wild-type RNAβ and mutant derivatives assayed with the dfBSMV derivative system. Red fluorescence resulting from the mCherry expression cassette identifies the primary infection foci, and green fluorescence resulting from γb-GFP expressed from the BSMV genome indicates the secondarily infected cells. TGB1-ΔN170 (Fig. 1C) was used as a movement-incompetent control. Arrows indicate virus movement. Bars, 200 μm. (C) Quantification of virus movement. The green fluorescence foci in 10 *N. benthamiana* epidermal leaves were quantified by ImageJ. Brackets and asterisks indicate statistical differences determined by an unpaired two-tailed Student's *t*-test. $^*P < 0.05$ (significant). (D) Systemically infected *N. benthamiana* plant symptoms photographed at 16 dpi. (E) Coat protein (CP) enzyme-linked immunosorbent assay (ELISA) of upper emerging leaves at 16 dpi.

designated NLS_A and NLS_B, which are located between amino acids 95 and 104 and 227 and 238, respectively (Fig. 4A). To obtain a more detailed characterization of the NLSs and NoLSs, the N-terminal 240-amino-acid fragment (N_{240}) of TGB1 and its single and double NLS mutants (Fig. 4B) were fused with GFP and used for LSCM experiments. Consistent with full-length TGB1, the N_{240}-GFP fusion protein localized to the cytoplasm, nucleus and nucleolus (Figs4C and S4, see Supporting Information). In contrast, the N_{240}Am-GFP fusion localized to the cytoplasm and nucleoplasm, but not to the nucleolus (Figs4C and S4). However, neither the N_{240}Bm or N_{240}ABm fusions accumulated in the nucleus (Figs4C and S4). Moreover, the TGB1 C-terminal 241–512-amino-acid (C_{272}-GFP) fusion formed bright punctate foci in the cytoplasm, but not in the nucleus, verifying that the C-terminus of TGB1 does not contain NLSs (Figs4C and S4). In summary, these results demonstrate that TGB1 contains a functional NoLS between amino acids 95 and 104, and a functional NLS between amino acids 227 and 238.

As nuclear-cytoplasmic trafficking of TGB1 is required for BSMV movement, we investigated the requirements of the NoLS and NLS domains for cell-to-cell movement and systemic infection. The TGB1 NoLS and NLS sequences were mutated to inactivate

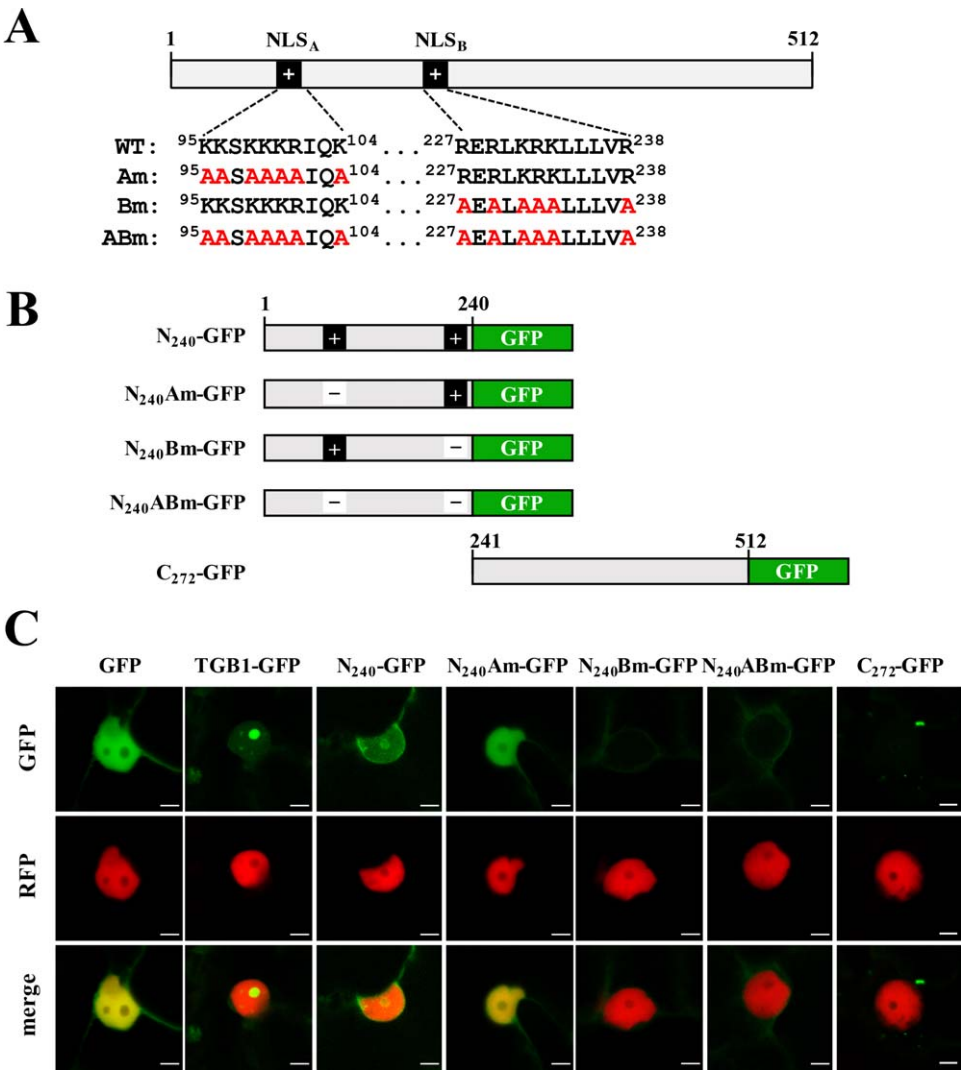

Fig. 4 Subcellular localization of Triple Gene Block1 (TGB1) mutants. (A) Diagram illustrating the TGB1 structure and sequences of the predicted and mutated nuclear localization signals (NLSs). (B) Depiction of the N-terminal and C-terminal domains of TGB1 fused with green fluorescent protein (GFP). (C) Nuclear localization of GFP (control), TGB1-GFP, N_{240}-GFP, N_{240}Am-GFP, N_{240}Bm-GFP, N_{240}ABm-GFP and C_{272}-GFP in agroinfiltrated leaves of transgenic *Nicotiana benthamiana* plants constitutively expressing H2B-RFP. The infiltrated regions of the leaves were photographed at 3 days post-infiltration (dpi). RFP, red fluorescent protein. Bars, 5 μm.

the respective localization signals. The WT and mutant BSMV derivatives were inoculated by agroinfiltration of *N. benthamiana* leaves, and the infiltrated regions were collected at 5 dpi for western blot analyses. The results indicated that the NoLS mutant ($BSMV_{mNoLS}$) had slightly lower TGB1 accumulation than WT BSMV; however, both the NLS mutant ($BSMV_{mNLS}$) and the NoLS/NLS double mutant viruses ($BSMV_{mNoLS/mNLS}$) had substantially lower TGB1 accumulation in the infiltrated leaf samples (Fig. 5A). To further determine the effects of the TGB1 NLS and NoLS mutants on BSMV cell-to-cell movement, the dfBSMV and dfBSMV derivatives were agroinfiltrated into *N. benthamiana* leaves and observed at 3 dpi. The $dfBSMV_{mNoLS}$ mutant virus was notably impaired in cell-to-cell movement, and the intercellular movement abilities of the $dfBSMV_{mNLS}$ and $dfBSMV_{mNoLS/mNLS}$ mutants were almost completely abolished (Fig. 5B,C). Furthermore, none of the mutants ($BSMV_{mNoLS}$, $BSMV_{mNLS}$ and $BSMV_{mNoLS/mNLS}$) were able to elicit *N. benthamiana* systemic symptoms (Fig. 5D and Table S3, see Supporting Information), and the visual observations were confirmed by ELISA (Fig. 5E) and RT-PCR detection (Fig. S3B). These results indicate that the mutations introduced into the NLS and NoLS motifs in TGB1 significantly impair or abolish BSMV cell-to-cell and long-distance movement in *N. benthamiana*.

We also evaluated the infectivity of the mutant BSMV viruses in the natural host, barley. The α, β and γ RNAs transcribed from BSMV infectious clones (Petty *et al.*, 1989) were mixed in equal amounts and inoculated onto barley at the two-leaf stage. Consistent with the *N. benthamiana* results, neither the $BSMV_{mNLS}$ nor $BSMV_{mNoLS/mNLS}$ mutants were able to infect barley systemically, but $BSMV_{mNoLS}$ was able to establish systemic barley infections (Fig. S5 and Table S3, see Supporting Information). Taken together, TGB1 NLS is required for viral intercellular and long-distance movement in both *N. benthamiana* and barley, but NoLS is required for viral long-distance movement in *N. benthamiana*, but not in barley.

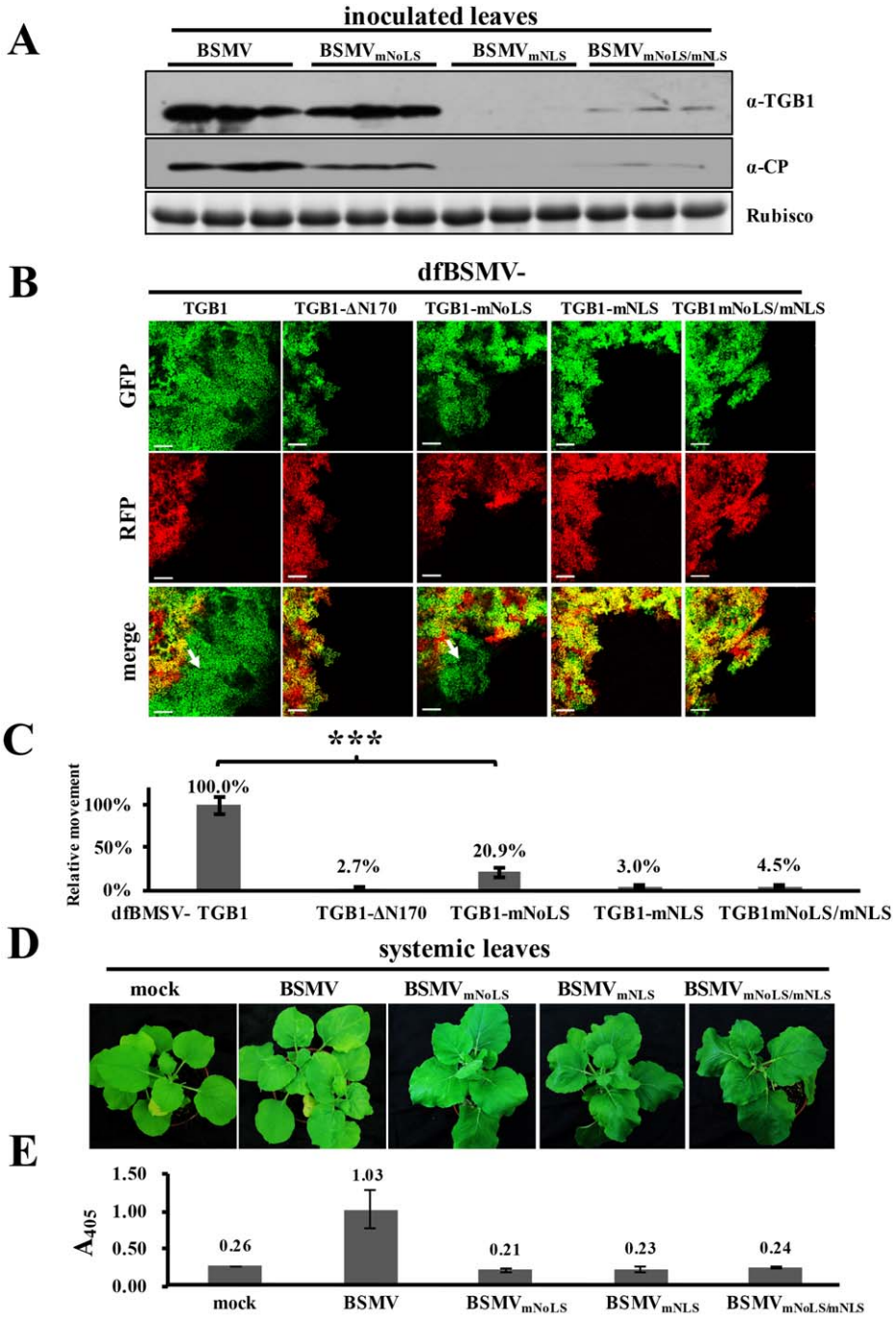

Fig. 5 Effects of Triple Gene Block1 (TGB1) nucleolar localization signal (NoLS) and nuclear localization signal (NLS) mutations on *Barley stripe mosaic virus* (BSMV) cell-to-cell and long-distance movement. (A) Western blot detection of coat protein (CP) and TGB1 accumulation of BSMV, BSMV NLS and BSMV NoLS mutants at 5 days after agroinfiltration of *Nicotiana benthamiana* leaves. Ribulose-1,5-bisphosphate carboxylase/oxygenase (Rubisco) levels indicate equal loading. (B) Cell-to-cell movement of dfBSMV and the dfBSMV mutants in agroinoculated *N. benthamiana* leaves at 3 days post-infiltration (dpi). Bars, 200 μm. Arrows indicate the directions of virus movement. GFP, green fluorescent protein; RFP, red fluorescent protein. (C) Quantification of cell-to-cell movement of dfBSMV and mutant viruses. The green fluorescent foci representing virus movement in 10 *N. benthamiana* samples were quantified by ImageJ. Brackets and asterisks show statistical differences determined by unpaired two-tailed Student's *t*-test. $***P < 0.001$ (extremely significant). (D) Symptoms of systemically infected *N. benthamiana* plants at 16 dpi. (E) CP enzyme-linked immunosorbent assay (ELISA) of systemically infected leaves.

Fib2 is involved in BSMV cell-to-cell movement

Previous reports have shown that Fib2 depletion prevents GRV systemic movement, but not replication or cell-to-cell movement (Kim *et al.*, 2007a). To examine Fib2 expression in BSMV-infected cells, western and northern blots were conducted with BSMV-infected leaf extracts collected at 12 dpi. Compared with heathy plants, Fib2 expression was up-regulated by about 60%–70% (Fig. 6A), implying that Fib2 could be involved in BSMV infection. To evaluate this proposition in more detail, the effect of transient *fib2* RNA silencing on BSMV infection in *N. benthamiana* was tested. For this purpose, a fragment of *fib2* was constructed in the forward and reverse orientations to generate hairpin structures and inserted into pMDC32 to create the RNAi-*fib2* plasmid (Fig. S6A, see Supporting Information). *Nicotiana benthamiana* leaves were then co-infiltrated with agrobacteria harbouring the BSMV plasmids and either the

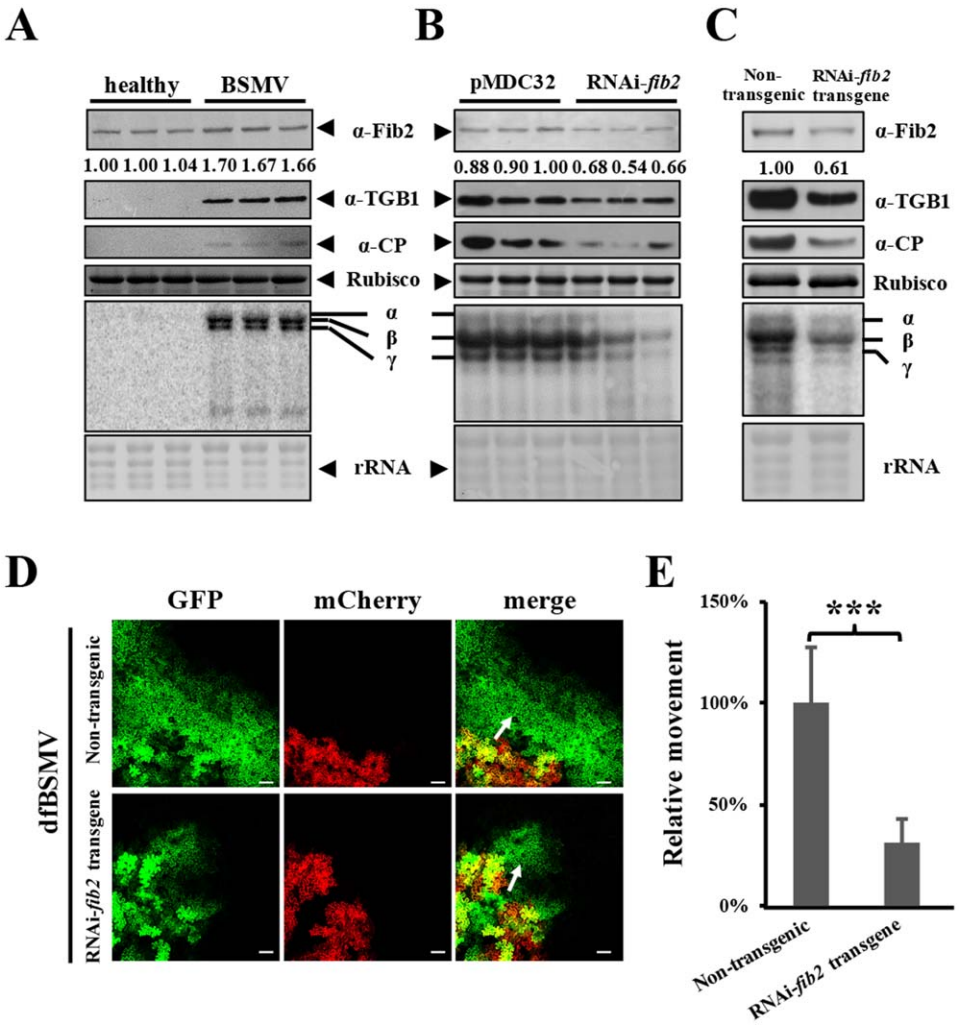

Fig. 6 Effects of fibrillarin (Fib2) expression on *Barley stripe mosaic virus* (BSMV) infection and *fib2* silencing on BSMV cell-to-cell movement. (A) Analysis of Fib2 expression in healthy and BSMV-infected leaves at 12 days post-infiltration (dpi). Fib2 expression was examined by western blotting with anti-Fib2 (α-Fib2), and band quantification. Western blot detection of Triple Gene Block1 (TGB1) and coat protein (CP) with their respective antibodies (α-) and northern blot detection of genomic RNAs (gRNAs) with the 3′-untranslated region (3′-UTR)-specific probe (Petty *et al.*, 1990) were used to show viral infection. (B) Effects of *fib2* silencing on BSMV protein and gRNA accumulation. The BSMV α, β and γ plasmids and RNAi-*fib2* or the control plasmid, pMDC32 (Curtis & Grossniklaus, 2003), were agroinfiltrated into *Nicotiana benthamiana* leaves, and analyses were conducted at 3 dpi. Ribulose-1,5-bisphosphate carboxylase/oxygenase (Rubisco) analysis verified equal sample loading. (C) Western and northern blot detection of BSMV accumulation in non-transgenic and RNAi-*fib2* transgenic plants at 3 dpi. (D) Cell-to-cell movement of dfBSMV in non-transgenic and RNAi-*fib2* transgenic plants. Arrows indicate the direction of virus movement. Bars, 100 μm. (E) Quantification of virus movement in non-transgenic and RNAi-*fib2* transgenic plants. The green fluorescent foci in 10 *N. benthamiana* epidermal leaves were quantified by ImageJ. Brackets and asterisks indicate statistical differences determined by an unpaired two-tailed Student's *t*-test. $***P < 0.001$ (extremely significant).

RNAi-*fib2* plasmid or the control pMDC32 vector, and the infiltrated leaf tissue was isolated at 3 dpi and evaluated for Fib2 and BSMV accumulation. The results revealed that the abundance of Fib2 was reduced by at least 30% in tissue infiltrated with RNAi-*fib2* compared with tissue infiltrated with pMDC32, and that the accumulation of BSMV, CP, TGB1 and viral RNAs was also reduced by about the same amount (Fig. 6B). Thus, these experiments suggest that there is a direct correlation between reductions in Fib2 abundance and BSMV infection.

To extend the transient *fib2* silencing results, the RNAi-*fib2* plasmid was used to engineer *N. benthamiana* transgenic plants expressing a hairpin RNA structure consisting of a portion of *fib2* RNA (Fig. S6). The RNAi-*fib2* transgenic plants were stunted compared with non-transgenic plants (Fig. S6B), and Fib2 accumulation was reduced by about 40%. BSMV accumulation was reduced in RNAi-*fib2* transgenic plants (Fig. 6C). Moreover, BSMV cell-to-cell movement in RNAi-*fib2* transgenic plants was also evaluated with the dfBSMV virus, and found to be less than one-

third of that of the non-transgenic plants (Fig. 6D,E). In summary, these data demonstrate that Fib2 is stimulated on BSMV infection and that Fib2 depletion suppresses dfBSMV cell-to-cell movement.

Fib2 interacts directly *in vitro* and *in vivo* with TGB1, but not with the TGB1 NLS mutants

To detect interactions between Fib2 and BSMV TGB1, BiFC assays were performed with transgenic plants constitutively expressing H2B-RFP to provide a nuclear marker. Different combinations of fusion proteins containing N- or C-terminally tagged YFP halves of TGB1 or Fib2 were tested for possible *in vivo* interactions. In these experiments, TGB1 interacted with Fib2 mainly in the nucleolus, but the NoLS and NLS mutants did not interact with Fib2 (Fig. 7A). These results imply that nucleolar localization of TGB1 is a prerequisite for Fib2 interactions, and that disruption of the NoLS or NLS motifs affects the ability to establish TGB1–Fib2 interactions. Moreover, co-immunoprecipitation (CoIP) experiments between Flag-TGB1 and Fib2-Myc indicate that these interactions are the result of direct TGB1–Fib2 binding (Fig. 7B).

Fib2 can be divided into four regions according to sequence characteristics (Rodriguez-Corona *et al.*, 2015), with one region containing the glycine–arginine-rich (GAR) domain functioning in interactions with various viral proteins (VPs) (Kim *et al.*, 2007b; Semashko *et al.*, 2012). Therefore, the Fib2, GAR domain and a truncation mutant ($Fib2_{\triangle GAR}$) were cloned into *E. coli* cells and purified. Affinity assays were performed with amylose resin, and GST-GFP and maltose-binding proteins (MBPs) were used as negative controls. The results showed that TGB1 can interact with full-length Fib2 and the GAR domain, and that interactions between TGB1 and the GAR domain are stronger than those between TGB1 and full-length Fib2 (Fig. 7C). Altogether, these data suggest that TGB1 interacts directly with Fib2 *in vivo* and *in vitro*, and that the TGB1 NoLS and NLS mutants do not interact with Fib2.

Fib2 interacts with the BSMV RNP

As TGB1 interacts directly with Fib2, we evaluated the co-localization of the two proteins. *Agrobacterium* strains expressing TGB1-GFP and Fib2-RFP were co-infiltrated into *N. benthamiana* leaves and examined by confocal microscopy at 3 dpi. The results showed that TGB1 co-localizes mainly in the nucleolus with Fib2, but we noticed that the two proteins also accumulate in the cytoplasm (Fig. 8A). To exclude non-specific expression of Fib2 in the cytoplasm, a control experiment co-expressing GFP and Fib2 was conducted to evaluate possible TGB1 effects on Fib2 localization. In this experiment, Fib2 localized to the nucleolus, whereas, as expected, GFP fluoresced in both the cytoplasm and nucleoplasm (Fig. S7, see Supporting Information). Thus, these data imply that Fib2 is redistributed from the nucleolus to the cytoplasm by TGB1 during BSMV infection. Co-localization of TGB1 and Fib2 in BSMV-infected cells was also tested. The α, $\beta_{GFP\text{-}TGB1}$ (Fig. 1C) and γ RNAs, together with Fib2-RFP, were transiently expressed in *N. benthamiana* via agroinfiltration. As expected, TGB1 and Fib2 co-localized in the nucleolus in the infected cells, but co-localization of the two proteins was also evident at the plasmodesmata (PD) (Fig. 8B, top and middle panels); however, Fib2 did not associate with PD when co-expressed with GFP (Fig. 8B, bottom panel). These findings indicate that Fib2 is redistributed from the nucleolus to the cytoplasm by TGB1, and that the Fib2–TGB1 complex may be involved in BSMV cell-to-cell movement. Because the BSMV RNP contains TGB1 and vRNAs (Lim *et al.*, 2008), we also tested whether Fib2 co-localizes with BSMV RNA. For this purpose, CitN-PUMHD3794, PUMHD3809-CitC (Tilsner *et al.*, 2009), TGB1-CFP and Fib2-RFP were co-expressed in $BSMV_{(+)\gamma bPUM}$-infected leaves (Zhang *et al.*, 2017). As anticipated, Fib2, TGB1 and vRNA co-localized near the cell wall (Fig. 8C). We propose that Fib2 is hijacked by TGB1 to interact with the BSMV RNP movement complex, and that Fib2, TGB1 and vRNA may be RNP components.

DISCUSSION

Our data demonstrate that BSMV TGB1 mainly localizes to the cytoplasm, but that a small fraction accumulates in the nucleus and nucleolus. TGB1 localization in these sites is required for viral cell-to-cell movement, and hence nuclear and nucleolar interactions are important in viral pathogenesis. Moreover, the nucleolar protein Fib2 also binds to TGB1 and may be a component of the BSMV RNP cell-to-cell movement complex.

Nuclear targeted proteins often contain arginine- and lysine-rich NLSs (Lange *et al.*, 2007) which interact with importin α/β proteins within the classical nuclear transport pathway (Gorlich & Kutay, 1999; Gorlich & Mattaj, 1996). Importin α binds to the NLS of cargo proteins and forms ternary complexes with importin β during nuclear transport (Goldfarb *et al.*, 2004). The mechanisms of protein transport to the nucleolus are obscure, but one hypothesis is that the NoLS may bind to a nucleolar protein designated for nucleolar delivery. Several plant VPs not only have an NLS, but also an NoLS (Kim *et al.*, 2007b; Rawlinson & Moseley, 2015; Salvetti & Greco, 2014; Taliansky *et al.*, 2010). For example, GRV ORF3 contains functional NLS and NoLS sequences; moreover, substitution of the NLS arginine residues with alanine abolishes ORF3 nuclear transit, whereas NoLS leucine mutations interfere with ORF3 nucleolar localization (Kim *et al.*, 2007b). PMTV TGB1 contains two NoLSs responsible for nucleolar localization (Lukhovitskaya *et al.*, 2015). In contrast, the PSLV TGB1 N-terminal domain (NTD) contains a putative NLS (Cluster A, amino acids 116–125) required for nuclear localization and a putative NoLS (Cluster B, amino acids 175–187), and mutations within these regions result in the redistribution of most of the NTD from the nucleolus to the nucleoplasm (Semashko *et al.*, 2012). In the

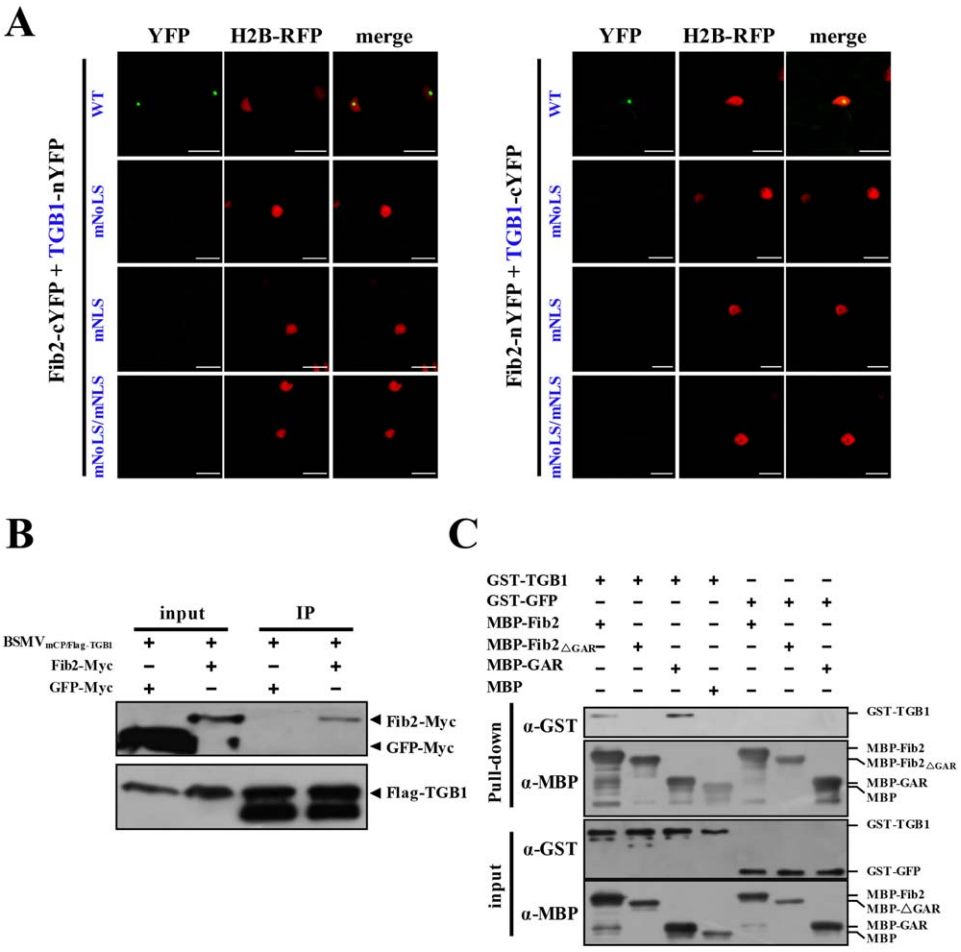

Fig. 7 Interactions between Triple Gene Block1 (TGB1) and fibrillarin (Fib2). (A) Bimolecular fluorescence complementation (BiFC) analyses of Fib2 interactions with TGB1 and the nucleolar (NoLS) and nuclear (NLS) localization signal mutations. Co-expression of Fib2-cYFP and TGB1-nYFP, or Fib2-nYFP and TGB1-cYFP, resulted in reconstitution of yellow fluorescent protein (YFP) fluorescence, but Fib2 co-expression with the TGB1 mutants failed to reconstitute YFP. Bars, 20 μm. (B) Co-immunoprecipitation of Flag-tagged TGB1 with Fib2. Agrobacteria containing α, γ, $\beta_{mCP/Flag\text{-}TGB1}$ (Fig. 1C) and Fib2-Myc, or GFP-Myc plasmids, were co-infiltrated into *Nicotiana benthamiana* leaves and extracts were analysed at 3 days post-infiltration (dpi). Myc and Flag antibodies were used in the western blots. (C) Maltose-binding protein (MBP) affinity assays between GST-TGB1 and MBP-Fib2 or the fib2 truncated mutants. GST-TGB1 was pulled down by MBP-Fib2 and MBP-GAR, but not by MBP-$Fib2_{\triangle GAR}$. GST-GFP and MBP were used as negative controls. GAR, glycine–arginine-rich domain; GFP, green fluorescent protein; GST, glutathione *S*-transferase.

current work, we have demonstrated that BSMV TGB1 has distinct NoLS (amino acids 95–104) and NLS (amino acids 227–238) regions. Multiple sequence alignments of TGB1 proteins show that both the NoLS and NLS are highly conserved amongst nine BSMV strains (Fig. S8, see Supporting Information). However, similar comparisons of BSMV, PSLV and *Lychnis ringspot virus* (LRSV) hordeivirus TGB1 proteins show that the NoLS is conserved, but the three hordeiviruses do not contain a conserved classical NLS (Fig. S9, see Supporting Information).

Several plant VPs that localize to the nucleus promote or inhibit infection (Hiscox, 2007; Taliansky *et al.*, 2010). The *Cucumber mosaic virus* (CMV) 2b silencing suppressor protein is targeted to the nucleolus by NLS1 and NLS2, and deletion of either one or both signals abolishes 2b local suppression of silencing (González *et al.*, 2010). Mutation of the CP NLS also abolishes BBSV transit to upper non-inoculated leaves (Zhang *et al.*, 2011, 2013). It is also relevant that nucleolar localization of GRV ORF3 is essential for the formation of viral RNPs and for systemic movement (Kim *et al.*, 2007b). PMTV TGB1 also contains two NoLSs, NoLS-A and NoLS-B. However, the NoLS-A and NoLS-B mutations do not affect viral accumulation in inoculated leaves, and the $NoLS\text{-}A^M$ mutant and WT virus accumulate to similar levels in the upper leaves, whereas accumulation of the $NoLS\text{-}B^M$ mutant is only slightly reduced (Lukhovitskaya *et al.*, 2015). Nevertheless, RNA-TGB1 of the double mutant virus, $NoLS\text{-}AB^M$, could be detected in the upper leaves, but RNA-CP could not be detected, and PMTV

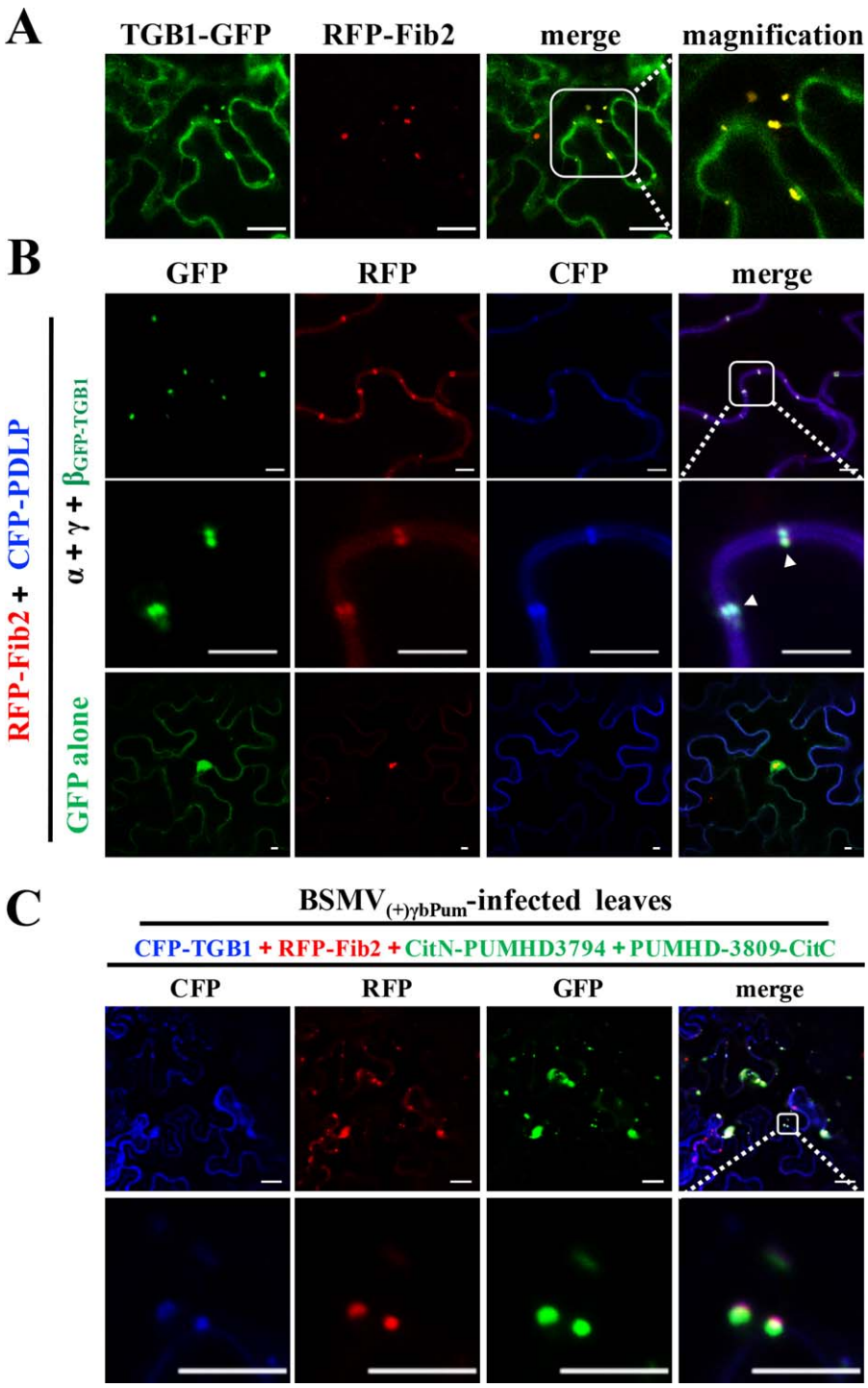

Fig. 8 Fibrillarin (Fib2) may be a component of the *Barley stripe mosaic virus* (BSMV) ribonucleoprotein. (A) Co-localization of Triple Gene Block1-green fluorescent protein (TGB1-GFP) and red fluorescent protein (RFP)-Fib2 during transient expression. The right panel shows the magnification of the white square. Bars, 20 μm. (B) Co-localization of RFP-Fib2 and GFP-TGB1 expressed during $BSMV_{GFP\text{-}TGB1}$ infection. *Agrobacterium* strains harbouring RFP-Fib2 and BSMV α, $\beta_{GFP\text{-}TGB1}$ and γ plasmids were co-infiltrated into *Nicotiana benthamiana* epidermal leaves, and confocal observations were performed at 3 days post-infiltration (dpi). Magnification of the white frame is shown in the middle panel. Cyan fluorescent protein (CFP)-PD-located protein (PDLP) was used as a marker of plasmodesmata. Co-localization of GFP and Fib2-RFP served as a negative control. Bars, 5 μm. (C) Co-localization of TGB1, Fib2 and BSMV plus-strand viral RNAs (vRNAs). CitN-PUMHD3794 and PUMHD3809-CitC (Tilsner *et al.*, 2009) were used to label the localization of BSMV plus-strand RNAs. Co-localization of CFP-TGB1, RFP-Fib2 and BSMV plus-strand RNAs was visualized in the upper systemically infected leaves of *N. benthamiana* plants infiltrated with $BSMV_{(+)\gamma bPum}$ derivatives (Zhang *et al.*, 2017). The bottom panel shows the magnification of the white square. Bars, 10 μm.

accumulation was greatly reduced, indicating that the NoLS motifs have synergistic effects on the systemic movement of RNA-CP (Lukhovitskaya *et al.*, 2015).

PSLV TGB1 has been reported to localize to the nucleus and nucleolus, but infectivity studies were not conducted (Semashko *et al.*, 2012). With BSMV, we found that TGB1 NoLS mutations reduced both virus accumulation and cell-to-cell movement in inoculated leaves, and that mutations affecting the NLS, or both the NoLS and NLS, significantly reduced BSMV accumulation in inoculated leaves and almost completely abolished cell-to-cell movement. Moreover, none of the mutant viruses were able to infect *N. benthamiana* systemically, but the NoLS mutant ($BSMV_{mNoLS}$)

was able to systemically infect barley. Hu *et al.* (2015) also reported similar observations with some of the BSMV TGB1 phosphorylation mutants in *N. benthamiana* versus barley and wheat. A possible explanation for this phenomenon is that the failure of $BSMV_{mNoLS}$ to infect *N. benthamiana* systemically versus its ability to infect barley may be the result of a requirement to move locally through the large number of cells separating the reticulated vasculature of dicots, compared with movement through the smaller number of cells separating the parallel vascular system of cereals. Hence, the mutant viruses normally would need to traverse fewer cells in monocots than in dicots to reach the vascular highway to the secondary leaves.

For many plant viruses, the RNP complex is the major form used to move across PD to neighbouring cells (Benitez-Alfonso *et al.*, 2010). The main components of viral RNPs are viral RNAs, MPs and CPs (Lucas *et al.*, 2009; Oparka *et al.*, 1997). In addition, some host factors are also involved in viral cell-to-cell and long-distance movement (Chen *et al.*, 2000; Harries *et al.*, 2009; Hipper *et al.*, 2013; Raffaele *et al.*, 2009; Semashko *et al.*, 2012; Taliansky *et al.*, 2010). Amongst these host factors are β-1,3-glucanases, remorin and Fib2, the main component of box C/D snoRNPs, which is the only methyltransferase found to direct 2′-*O*-ribose methylation of rRNA (Reichow *et al.*, 2007; Venema & Tollervey, 1999). The *Tobacco mosaic virus* (TMV) MP recruits β-1,3-glucanases to PD to degrade callose, which increases PD size exclusion limits (SEL) (Lee & Lu, 2011). As another example, *Potato virus X* (PVX) TGB1 interacts with remorin, a Solanaceae protein resident in PD and membrane rafts (Raffaele *et al.*, 2009). Several plant virus proteins also interact with Fib2, the main nucleolar protein (Taliansky *et al.*, 2010). ORF3, encoded by the umbravirus GRV, is a long-distance movement factor facilitating the trafficking of viral RNA through the phloem (Ryabov *et al.*, 1999). Umbraviruses do not encode a CP, and so formation of a viral RNP instead of virus particles functions in long-distance movement (Ryabov *et al.*, 1999). GRV ORF3 is targeted to the Cajal bodies and interacts with Fib2 to partially relocalize the protein from the nucleolus to the cytoplasm. Moreover, *fib2* silencing affects long-distance movement of GRV, but not TMV or PVX (Kim *et al.*, 2007a,b); thus, these viruses may differ mechanistically in interactions with host components involved in movement.

We found that BSMV TGB1 interacts directly with Fib2 via the GAR domain, and that abolishing these interactions results in the depletion of TGB1 from the nuclei and nucleoli. Therefore, interactions with Fib2 may provide a general mechanism for the targeting of various plant VPs to the nucleolus; however, comparison with other viruses indicates that the outcome of these interactions may differ depending on the virus. We also observed that, after BSMV infection, Fib2 was induced to about 60%–70% of that in healthy plants, and that transient expression of a *fib2* hairpin to induce *fib2* silencing affected BSMV accumulation in inoculated leaves and reduced BSMV cell-to-cell movement. Moreover, BSMV accumulation and cell-to-cell movement were reduced in RNAi-Fib2 transgenic plants compared with non-transgenic plants. We also found that Fib2 co-localized with TGB1 at the PD of BSMV-infected cells, and that Fib2 co-localized with BSMV vRNA and TGB1 (Fig. 8C), indicating that Fib2 may be a component of the BSMV RNP.

Based on our data and published results with other viruses, we present a general model illustrating the role of Fib2 in virus cell-to-cell and long-distance movement (Fig. 9). Different VPs, such as satBaMV P20 (Chang *et al.*, 2016), RSV P2 (Zheng *et al.*, 2015), hordei-like TGB1s (Lukhovitskaya *et al.*, 2015; Semashko *et al.*, 2012), BBSV p7a (Wang *et al.*, 2012), PVA VPg (Rajamaki & Valkonen, 2009) and GRV ORF3 (Kim *et al.*, 2007a,b), traffic to the nucleolus via interactions with the importin α/β or other pathway. These diverse VPs interact with Fib2 in the nucleolus and initiate the formation of viral RNP (vRNP) complex intermediates that are transported to the cytoplasm (Fig. 9A). In BSMV, the nascent movement complexes then interact with viral RNAs, TGB2 and TGB3 to complete vRNP assembly in conjunction with chloroplast vesicles where BSMV replication occurs (Jin *et al.*, 2017; Lin & Langenberg, 1985; Torrance *et al.*, 2006; Zhang *et al.*, 2017). The movement complexes are then transported to the PD via proliferated endoplasmic reticulum (ER) vesicles and actin cytoskeleton interactions (Lim *et al.*, 2013; Verchot-Lubicz *et al.*, 2010), and move from cell to cell to vascular elements to achieve long-distance movement. Other viral movement complexes in the genera *Potexvirus*, *Umbravirus* and *Potyvirus* may also carry out cytoplasmic aspects of cell-to-cell movement via different pathways (Chang *et al.*, 2016; Kim *et al.*, 2007a,b; Rajamaki & Valkonen, 2009). Previous reports provide evidence suggesting that Fib2 is involved in the long-distance movement of several viruses because Fib2 knockdowns or depletions affect systemic movement, but not cell-to-cell movement (Chang *et al.*, 2016; Kim *et al.*, 2007a; Rajamaki & Valkonen, 2009; Zheng *et al.*, 2015) (Fig. 9B). Here, we show that Fib2 is critical for BSMV cell-to-cell movement. In conclusion, our results provide increasing evidence that Fib2 interactions during virus infection not only affect long-distance movement, but may also be an essential requirement for cell-to-cell movement.

EXPERIMENTAL PROCEDURES

Plasmid constructions

Details on plasmid constructions are presented in Text S1 (see Supporting Information).

Confocal microscopy

Confocal microscopy was performed using a Zeiss LSM710 confocal microscope (Carl Zeiss 710, Germany) with a 63× oil immersion objective lens

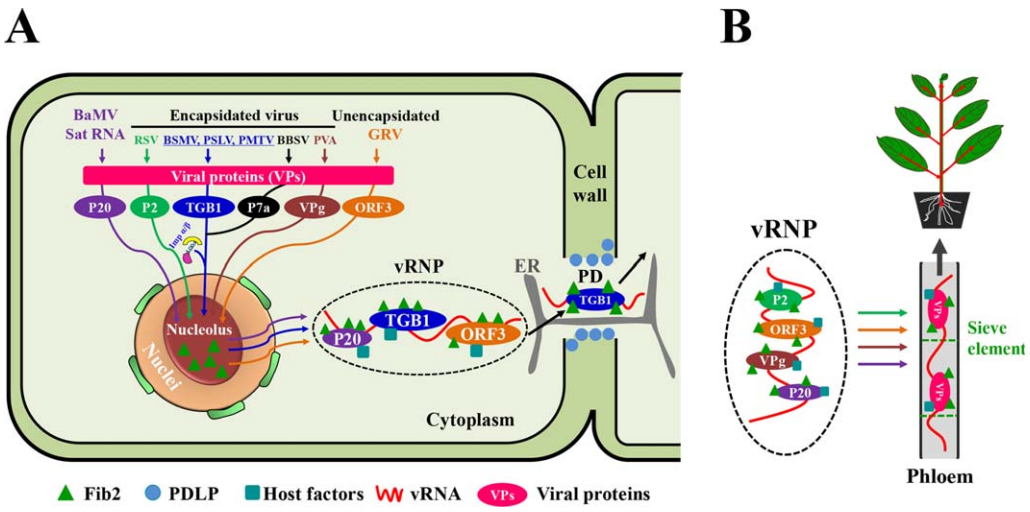

Fig. 9 Model for the role of fibrillarin (Fib2) in viral cell-to-cell (A) and long-distance (B) movement. (A) The viruses that have been reported to interact with Fib2 were classified into three types: encapsidated viruses, unencapsidated viruses and viruses with satellite RNAs. First, the viral proteins (VPs) P20, P2, Triple Gene Block1 (TGB1), P7a, VPg and ORF3 are translated in the cytoplasm and a portion of the population is transported into the nucleolus by the importin α/β pathway. These viral proteins bind to Fib2 in the nucleolus and are imported from the nucleus to the cytoplasm to form viral ribonucleoprotein (vRNP) constituents. The movement of vRNPs consists of viral-encoded movement proteins and the viral gRNAs, Fib2, host factors and possibly various other virus-encoded proteins. For *Barley stripe mosaic virus* (BSMV), the vRNP, including Fib2, is involved in virus cell-to-cell movement. (B) The other vRNP or virions including Fib2 and ORF3, P20, P2 or VPg function in long-distance movement and are loaded into the phloem. BaMV, *Bamboo mosaic virus*; BBSV, *Beet black scorch virus*; ER, endoplasmic reticulum; GRV, *Groundnut rosette virus*; PD, plasmodesmata; PMTV, *Potato mop-top virus*; PSLV, *Poa semilatent virus*; PVA, *Potato virus A*; RSV, *Rice stripe virus*; PDLP, PD-located protein.

(NA 1.2) or a 40× water immersion objective lens (NA 1.2). Excitation wavelengths were as follows: CFP, 440 nm; GFP, 488 nm; YFP, 514 nm; RFP, 561 nm. Detection bands were optimized for each fluorophore group to avoid emission bleeding.

Isolation of plant nuclei

Two grams of BSMV-infected and healthy *N. benthamiana* leaves were harvested and nuclear isolations were performed with a plant nuclei isolation/extraction kit (Sigma Aldrich, USA) according to the technical instructions (Lee *et al.*, 1988; Luthe & Quatrano, 1980) provided by the manufacturer. The purity of the cytoplasmic and nuclear fractions was determined by western blotting with the phosphoenolpyruvate carboxylase (PEPC) (Cell Signaling Technology, Massachusetts, USA) cytoplasmic marker and the histone 3 (H3) nuclear marker, respectively.

Immunogold labelling

Immunogold labelling was performed according to a method described previously (Bendayan & Zollinger, 1983). The TGB1 antibody (Hu *et al.*, 2015) was diluted 1 : 2000 and the anti-rabbit secondary antibody conjugated with 10-nm gold particles (Sigma Aldrich) was diluted 1 : 20. The samples were examined with a Hitachi H-7650 electron microscope (Hitachi, Japan).

MBP affinity assays

MBP-Fib2, MBP-GAR and MBP-Fib2$_{\Delta GAR}$ proteins were expressed and purified from BL21(DE3) pLysS cells (Novagene, USA) by standard protocols. MBP pull-down assays were performed as described previously (Wissmann *et al.*, 2007).

Co-IP assays

Co-IPs were performed according to previously published protocols (Hu *et al.*, 2015; Rubio *et al.*, 2005). Inoculated *N. benthamiana* leaves were harvested at 3 dpi and Co-IP assays were performed on the leaf extracts.

Generation of RNAi-*fib2* transgenic plants

The plasmid RNAi-*fib2* was introduced into *Agrobacterium* strain EHA105, and transformation of *N. benthamiana* plants was carried out by a leaf disc method as described previously (Horsch *et al.*, 1989). Genomic DNA from regenerated plants was extracted with a cetyltrimethylammonium bromide (CTAB) method (Doyle & Doyle, 1987) and subjected to PCR analysis to screen positive transgenic plants.

ACKNOWLEDGEMENTS

We thank Dr Andrew O. Jackson (University of California at Berkeley, CA, USA) for constructive criticism and helpful editorial suggestions, and members of the Li laboratory for useful and crucial discussions. We would also like to thank Dr Xiaorong Tao (Nanjing Agricultural University, Nanjing, China) for the pCB301-2x35S-MCS-HDVRz-NOS vector, and Dr Michael M. Goodin (University of Kentucky, Lexington, KY, USA) for H2B-RFP transgenic *Nicotiana benthamiana* seeds. This work was supported by the National Natural Science Foundation of China (31570143 and 31270184) and the Innovative Project of SKLAB (2017SKLAB1–6) to DL, and the Fundamental Research Funds for the Central Universities (2017SY003) to YZ.

REFERENCES

Banerjee, R., Weidman, M.K., Navarro, S., Comai, L. and Dasgupta, A. (2005) Modifications of both selectivity factor and upstream binding factor contribute to poliovirus-mediated inhibition of RNA polymerase I transcription. *J. Gen. Virol.* **86**, 2315–2322.

Bendayan, M. and Zollinger, M. (1983) Ultrastructural localization of antigenic sites on osmium-fixed tissues applying the protein A-gold technique. *J. Histochem. Cytochem.* **31**, 101–109.

Benitez-Alfonso, Y., Faulkner, C., Ritzenthaler, C. and Maule, A.J. (2010) Plasmodesmata: gateways to local and systemic virus infection. *Mol. Plant–Microbe Interact.* **23**, 1403–1412.

Bevington, J.M., Needham, P.G., Verrill, K.C., Collaco, R.F., Basrur, V. and Trempe, J.P. (2007) Adeno-associated virus interactions with B23/Nucleophosmin: identification of sub-nucleolar virion regions. *Virology*, **357**, 102–113.

Boisvert, F.M., van Koningsbruggen, S., Navascues, J. and Lamond, A.I. (2007) The multifunctional nucleolus. *Nat. Rev. Mol. Cell Biol.* **8**, 574–585.

Bragg, J.N. and Jackson, A.O. (2004) The C-terminal region of the *Barley stripe mosaic virus* γb protein participates in homologous interactions and is required for suppression of RNA silencing. *Mol. Plant Pathol.* **5**, 465–481.

Bragg, J.N., Lim, H.S. and Jackson, A.O. (2008) *Hordeivirus*. In: *Encyclopedia of Virology* (Mahy, B.W.J. and van Regenmortel, M.H.V., eds.), pp. 459–467. Oxford: Academic Press.

Canetta, E., Kim, S.H., Kalinina, N.O., Shaw, J., Adya, A.K., Gillespie, T., Brown, J.W.S. and Taliansky, M. (2008) A plant virus movement protein forms ringlike complexes with the major nucleolar protein, fibrillarin, *in vitro*. *J. Mol. Biol.* **376**, 932–937.

Chang, C.-H., Hsu, F.-C., Lee, S.-C., Lo, Y.-S., Wang, J.-D., Shaw, J., Taliansky, M., Chang, B.-Y., Hsu, Y.-H. and Lin, N.-S. (2016) The nucleolar fibrillarin protein is required for helper virus-independent long-distance trafficking of a subviral satellite RNA in plants. *Plant Cell*, **28**, 2586–2602.

Chen, M.H., Sheng, J., Hind, G., Handa, A.K. and Citovsky, V. (2000) Interaction between the *Tobacco mosaic virus* movement protein and host cell pectin methylesterases is required for viral cell-to-cell movement. *EMBO J.* **19**, 913–920.

Cui, Y., Lee, M.Y., Huo, N., Bragg, J., Yan, L., Yuan, C., Li, C., Holditch, S.J., Xie, J., Luo, M.-C., Li, D., Yu, J., Martin, J., Schackwitz, W., Gu, Y.Q., Vogel, J.P., Jackson, A.O., Liu, Z. and Garvin, D.F. (2012) Fine mapping of the *Bsr1 Barley stripe mosaic virus* resistance gene in the model grass *Brachypodium distachyon*. *PLoS One*, **7**, e38333.

Curtis, M.D. and Grossniklaus, U. (2003) A gateway cloning vector set for high-throughput functional analysis of genes in planta. *Plant Physiol.* **133**, 462–469.

Donald, R.G.K., Lawrence, D.M. and Jackson, A.O. (1997) The *Barley stripe mosaic virus* 58-kilodalton βb protein is a multifunctional RNA binding protein. *J. Virol.* **71**, 1538–1546.

Doyle, J. and Doyle, J. (1987) Genomic plant DNA preparation from fresh tissue—CTAB method. *Phytochem Bull.* **19**, 11–15.

Dubois, M.-L. and Boisvert, F.-M. (2016) The nucleolus: structure and function. In: *The Functional Nucleus* (Bazett-Jones, D.P. and Dellaire, G., eds.), pp. 29–49. Cham: Springer International Publishing.

Dundr, M. and Misteli, T. (2001) Functional architecture in the cell nucleus. *Biochem. J.* **356**, 297–310.

Goldfarb, D.S., Corbett, A.H., Mason, D.A., Harreman, M.T. and Adam, S.A. (2004) Importin α: a multipurpose nuclear-transport receptor. *Trends Cell Biol.* **14**, 505–514.

González, I., Martínez, L., Rakitina, D.V., Lewsey, M.G., Atencio, F.A., Llave, C., Kalinina, N.O., Carr, J.P., Palukaitis, P. and Canto, T. (2010) *Cucumber mosaic virus* 2b protein subcellular targets and interactions: their significance to RNA silencing suppressor activity. *Mol. Plant–Microbe Interact.* **23**, 294–303.

Gorlich, D. and Kutay, U. (1999) Transport between the cell nucleus and the cytoplasm. *Annu. Rev. Cell Dev. Biol.* **15**, 607–660.

Gorlich, D. and Mattaj, I.W. (1996) Nucleocytoplasmic transport. *Science*, **271**, 1513–1518.

Greco, A. (2009) Involvement of the nucleolus in replication of human viruses. *Rev. Med. Virol.* **19**, 201–214.

Harries, P.A., Park, J.W., Sasaki, N., Ballard, K.D., Maule, A.J. and Nelson, R.S. (2009) Differing requirements for actin and myosin by plant viruses for sustained intercellular movement. *Proc. Natl. Acad. Sci. USA*, **106**, 17 594–17 599.

Hellen, C.U. and Sarnow, P. (2001) Internal ribosome entry sites in eukaryotic mRNA molecules. *Genes Dev.* **15**, 1593–1612.

Hipper, C., Brault, V., Ziegler-Graff, V. and Revers, F. (2013) Viral and cellular factors involved in phloem transport of plant viruses. *Front. Plant Sci.* **4**, 154.

Hiscox, J.A. (2007) RNA viruses: hijacking the dynamic nucleolus. *Nat. Rev. Microbiol.* **5**, 119–127.

Horsch, R.B., Fry, J., Hoffmann, N., Neidermeyer, J., Rogers, S.G. and Fraley, R.T. (1989) Leaf disc transformation. In: *Plant Molecular Biology Manual* (Gelvin, S.B., Schilperoort, R.A. and Verma, D.P.S., eds.), pp. 63–71. Dordrecht: Springer.

Hu, Y., Li, Z., Yuan, C., Jin, X., Yan, L., Zhao, X., Zhang, Y., Jackson, A.O., Wang, X., Han, C., Yu, J. and Li, D. (2015) Phosphorylation of TGB1 by protein kinase CK2 promotes *Barley stripe mosaic virus* movement in monocots and dicots. *J. Exp. Bot.* **66**, 4733–4747.

Jackson, A.O., Lim, H.S., Bragg, J., Ganesan, U. and Lee, M.Y. (2009) Hordeivirus replication, movement, and pathogenesis. *Annu. Rev. Phytopathol.* **47**, 385–422.

Jin, X., Jiang, Z., Zhang, K., Wang, P., Cao, X., Yue, N., Wang, X., Zhang, X., Li, Y., Li, D., Kang, B.H. and Zhang, Y. (2017) Three-dimensional analysis of chloroplast structures associated with virus infection. *Plant Physiol.* in press. doi: 10.1104/pp.17.00871.

Kalderon, D., Roberts, B.L., Richardson, W.D. and Smith, A.E. (1984) A short amino acid sequence able to specify nuclear location. *Cell*, **39**, 499–509.

Kalinina, N.O., Rakitina, D.V., Solovyev, A.G., Schiemann, J. and Morozov, S.Y. (2002) RNA helicase activity of the plant virus movement proteins encoded by the first gene of the triple gene block. *Virology*, **296**, 321–329.

Kim, S.H., Macfarlane, S., Kalinina, N.O., Rakitina, D.V., Ryabov, E.V., Gillespie, T., Haupt, S., Brown, J.W.S. and Taliansky, M. (2007a) Interaction of a plant virus-encoded protein with the major nucleolar protein fibrillarin is required for systemic virus infection. *Proc. Natl. Acad. Sci. USA*, **104**, 11 115–11 120.

Kim, S.H., Ryabov, E.V., Kalinina, N.O., Rakitina, D.V., Gillespie, T., MacFarlane, S., Haupt, S., Brown, J.W.S. and Taliansky, M. (2007b) Cajal bodies and the nucleolus are required for a plant virus systemic infection. *EMBO J.* **26**, 2169–2179.

Kosugi, S., Hasebe, M., Tomita, M. and Yanagawa, H. (2009) Systematic identification of cell cycle-dependent yeast nucleocytoplasmic shuttling proteins by prediction of composite motifs. *Proc. Natl. Acad. Sci. USA*, **106**, 10 171–10 176.

Lanford, R.E. and Butel, J.S. (1984) Construction and characterization of an SV40 mutant defective in nuclear transport of T antigen. *Cell*, **37**, 801–813.

Lange, A., Mills, R.E., Lange, C.J., Stewart, M., Devine, S.E. and Corbett, A.H. (2007) Classical nuclear localization signals: definition, function, and interaction with importin α. *J. Biol. Chem.* **282**, 5101–5105.

Lawrence, D.M. and Jackson, A.O. (2001a) Interactions of the TGB1 protein during cell-to-cell movement of *Barley stripe mosaic virus*. *J. Virol.* **75**, 8712–8723.

Lawrence, D.M. and Jackson, A.O. (2001b) Requirements for cell-to-cell movement of *Barley stripe mosaic virus* in monocot and dicot hosts. *Mol. Plant Pathol.* **2**, 65–75.

Lee, J.Y. and Lu, H. (2011) Plasmodesmata: the battleground against intruders. *Trends Plant Sci.* **16**, 201–210.

Lee, K.A.W., Bindereif, A. and Green, M.R. (1988) A small-scale procedure for preparation of nuclear extracts that support efficient transcription and pre-mRNA splicing. *Gene Anal. Tech.* **5**, 22–31.

Lee, M.Y., Yan, L., Gorter, F.A., Kim, B.Y.T., Cui, Y., Hu, Y., Yuan, C., Grindheim, J., Ganesan, U., Liu, Z., Han, C., Yu, J., Li, D. and Jackson, A.O. (2012) *Brachypodium distachyon* line Bd3-1 resistance is elicited by the barley stripe mosaic virus triple gene block 1 movement protein. *J. Gen. Virol.* **93**, 2729–2739.

Lim, H.-S., Bragg, J.N., Ganesan, U., Lawrence, D.M., Yu, J., Isogai, M., Hammond, J. and Jackson, A.O. (2008) Triple gene block protein interactions involved in movement of *Barley stripe mosaic virus*. *J. Virol.* **82**, 4991–5006.

Lim, H.-S., Bragg, J.N., Ganesan, U., Ruzin, S., Schichnes, D., Lee, M.Y., Vaira, A.M., Ryu, K.H., Hammond, J. and Jackson, A.O. (2009) Subcellular localization of the *Barley stripe mosaic virus* triple gene block proteins. *J. Virol.* **83**, 9432–9448.

Lim, H.-S., Lee, M.Y., Moon, J.S., Moon, J.-K., Yu, Y.-M., Cho, I.S., Bae, H., DeBoer, M., Ju, H., Hammond, J. and Jackson, A.O. (2013) Actin cytoskeleton and Golgi involvement in *Barley stripe mosaic virus* movement and cell wall localization of triple gene block proteins. *Plant Pathol J.* **29**, 17–30.

Lin, N.S. and Langenberg, W.G. (1985) Peripheral vesicles in proplastids of barley stripe mosaic virus-infected wheat cells contain double-stranded RNA. *Virology*, **142**, 291–298.

Lucas, W.J., Ham, B.K. and Kim, J.Y. (2009) Plasmodesmata – bridging the gap between neighboring plant cells. *Trends Cell Biol.* **19**, 495–503.

Lukhovitskaya, N.I., Cowan, G.H., Vetukuri, R.R., Tilsner, J., Torrance, L. and Savenkov, E.I. (2015) Importin-alpha-mediated nucleolar localization of *Potato mop-top virus* TRIPLE GENE BLOCK1 (TGB1) protein facilitates virus systemic movement, whereas TGB1 self-interaction is required for cell-to-cell movement in *Nicotiana benthamiana*. *Plant Physiol.* **167**, 738–752.

Luthe, D.S. and Quatrano, R.S. (1980) Transcription in isolated wheat nuclei: I. Isolation of nuclei and elimination of endogenous ribonuclease activity. *Plant Physiol.* **65**, 305–308.

Martin, K., Kopperud, K., Chakrabarty, R., Banerjee, R., Brooks, R. and Goodin, M.M. (2009) Transient expression in *Nicotiana benthamiana* fluorescent marker lines provides enhanced definition of protein localization, movement and interactions in planta. *Plant J.* **59**, 150–162.

Matera, A.G., Izaguire-Sierra, M., Praveen, K. and Rajendra, T.K. (2009) Nuclear bodies: random aggregates of sticky proteins or crucibles of macromolecular assembly?. *Dev. Cell*, **17**, 639–647.

Matthews, D.A. (2001) Adenovirus protein V induces redistribution of nucleolin and B23 from nucleolus to cytoplasm. *J. Virol.* **75**, 1031–1038.

Morozov, S.Y. and Solovyev, A.G. (2003) Triple gene block: modular design of a multifunctional machine for plant virus movement. *J. Gen. Virol.* **84**, 1351–1366.

Oparka, K.J., Prior, D.A.M., SantaCruz, S., Padgett, H.S. and Beachy, R.N. (1997) Gating of epidermal plasmodesmata is restricted to the leading edge of expanding infection sites of tobacco mosaic virus (TMV). *Plant J.* **12**, 781–789.

Petty, I.T., Hunter, B.G., Wei, N. and Jackson, A.O. (1989) Infectious *Barley stripe mosaic virus* RNA transcribed in vitro from full-length genomic cDNA clones. *Virology*, **171**, 342–349.

Petty, I.T., French, R., Jones, R.W. and Jackson, A.O. (1990) Identification of *Barley stripe mosaic virus* genes involved in viral RNA replication and systemic movement. *EMBO J.* **9**, 3453–3457.

Raffaele, S., Bayer, E., Lafarge, D., Cluzet, S., German Retana, S., Boubekeur, T., Leborgne-Castel, N., Carde, J.-P., Lherminier, J., Noirot, E., Satiat-Jeunemaitre, B., Laroche-Traineau, J., Moreau, P., Ott, T., Maule, A.J., Reymond, P., Simon-Plas, F., Farmer, E.E., Bessoule, J.-J. and Mongrand, S. (2009) Remorin, a Solanaceae protein resident in membrane rafts and plasmodesmata, impairs *Potato virus X* movement. *Plant Cell*, **21**, 1541–1555.

Rajamaki, M.L. and Valkonen, J.P. (2009) Control of nuclear and nucleolar localization of nuclear inclusion protein a of picorna-like *Potato virus A* in *Nicotiana* species. *Plant Cell*, **21**, 2485–2502.

Rawlinson, S.M. and Moseley, G.W. (2015) The nucleolar interface of RNA viruses. *Cell. Microbiol.* **17**, 1108–1120.

Reichow, S.L., Hamma, T., Ferre-D'Amare, A.R. and Varani, G. (2007) The structure and function of small nucleolar ribonucleoproteins. *Nucleic Acids Res.* **35**, 1452–1464.

Rodriguez-Corona, U., Sobol, M., Rodriguez-Zapata, L.C., Hozak, P. and Castano, E. (2015) Fibrillarin from archaea to human. *Biol. Cell*, **107**, 159–174.

Rubio, V., Shen, Y., Saijo, Y., Liu, Y., Gusmaroli, G., Dinesh-Kumar, S.P. and Deng, X.W. (2005) An alternative tandem affinity purification strategy applied to Arabidopsis protein complex isolation. *Plant J.* **41**, 767–778.

Ryabov, E.V., Robinson, D.J. and Me, T. (1999) A plant virus encoded protein facilitates long-distance movement of heterologous viral RNA. *Proc. Natl. Acad. Sci. USA*, **96**, 1212–1217.

Salvetti, A. and Greco, A. (2014) Viruses and the nucleolus: the fatal attraction. *Biochim. Biophys. Acta*, **1842**, 840–847.

Semashko, M.A., González, I., Shaw, J., Leonova, O.G., Popenko, V.I., Taliansky, M.E., Canto, T. and Kalinina, N.O. (2012) The extreme N-terminal domain of a hordeivirus TGB1 movement protein mediates its localization to the nucleolus and interaction with fibrillarin. *Biochimie*, **94**, 1180–1188.

Slootweg, E., Roosien, J., Spiridon, L.N., Petrescu, A.-J., Tameling, W., Joosten, M., Pomp, R., van Schaik, C., Dees, R., Borst, J.W., Smant, G., Schots, A., Bakker, J. and Goverse, A. (2010) Nucleocytoplasmic distribution is required for activation of resistance by the potato NB-LRR receptor Rx1 and is balanced by its functional domains. *Plant Cell*, **22**, 4195–4215.

Taliansky, M.E., Brown, J.W.S., Rajamäki, M.L., Valkonen, J.P.T. and Kalinina, N.O. (2010) Involvement of the plant nucleolus in virus and viroid infections: parallels with animal pathosystems. In: *Advances in Virus Research* (Maramorosch, K., Shatkin, A.J. and Frederick, A.M., eds.), pp. 119–158. Burlington, MA: Academic Press.

Tilsner, J., Linnik, O., Christensen, N.M., Bell, K., Roberts, I.M., Lacomme, C. and Oparka, K.J. (2009) Live-cell imaging of viral RNA genomes using a Pumilio-based reporter. *Plant J.* **57**, 758–770.

Torrance, L., Cowan, G.H., Gillespie, T., Ziegler, A. and Lacomme, C. (2006) Barley stripe mosaic virus-encoded proteins triple-gene block 2 and gammab localize to chloroplasts in virus-infected monocot and dicot plants, revealing hitherto-unknown roles in virus replication. *J. Gen. Virol.* **87**, 2403–2411.

Venema, J. and Tollervey, D. (1999) Ribosome synthesis in *Saccharomyces cerevisiae*. *Annu. Rev. Genet.* **33**, 261–311.

Verchot-Lubicz, J., Torrance, L., Solovyev, A.G., Morozov, S.Y., Jackson, A.O. and Gilmer, D. (2010) Varied movement strategies employed by triple gene block-encoding viruses. *Mol. Plant–Microbe Interact.* **23**, 1231–1247.

Waggoner, S. and Sarnow, P. (1998) Viral ribonucleoprotein complex formation and nucleolar-cytoplasmic relocalization of nucleolin in poliovirus-infected cells. *J. Virol.* **72**, 6699–6709.

Wang, X., Zhang, Y., Xu, J., Shi, L., Fan, H., Han, C., Li, D. and Yu, J. (2012) The R-rich motif of *Beet black scorch virus* P7a movement protein is important for the nuclear localization, nucleolar targeting and viral infectivity. *Virus Res.* **167**, 207–218.

Wen, W., Meinkoth, J.L., Tsien, R.Y. and Taylor, S.S. (1995) Identification of a signal for rapid export of proteins from the nucleus. *Cell*, **82**, 463–473.

Wissmann, M., Yin, N., Müller, J.M., Greschik, H., Fodor, B.D., Jenuwein, T., Vogler, C., Schneider, R., Günther, T., Buettner, R., Metzger, E. and Schüle, R. (2007) Cooperative demethylation by JMJD2C and LSD1 promotes androgen receptor-dependent gene expression. *Nat. Cell Biol.* **9**, 347–353.

Yao, M., Zhang, T., Tian, Z., Wang, Y. and Tao, X. (2011) Construction of agrobacterium-mediated *Cucumber mosaic virus* infectious cDNA clones and 2b deletion viral vector. *Sci. Agric. Sin.* **44**, 3060–3068.

Yelina, N.E., Savenkov, E.I., Solovyev, A.G., Morozov, S.Y. and Valkonen, J.P.T. (2002) Long-distance movement, virulence, and RNA silencing suppression controlled by a single protein in hordei- and potyviruses: complementary functions between virus families. *J. Virol.* **76**, 12 981–12 991.

Zhang, K., Zhang, Y., Yang, M., Liu, S., Li, Z., Wang, X., Han, C., Yu, J., Li, D. and Dinesh-Kumar, S.P. (2017) The *Barley stripe mosaic virus* γb protein promotes chloroplast-targeted replication by enhancing unwinding of RNA duplexes. *PLoS Pathog.* **13**, e1006319.

Zhang, X., Zhao, X., Zhang, Y., Niu, S., Qu, F., Zhang, Y., Han, C., Yu, J. and Li, D. (2013) N-terminal basic amino acid residues of *Beet black scorch virus* capsid protein play a critical role in virion assembly and systemic movement. *Virol J.* **10**, 200.

Zhang, Y., Zhang, X., Niu, S., Han, C., Yu, J. and Li, D. (2011) Nuclear localization of *Beet black scorch virus* capsid protein and its interaction with importin α. *Virus Res.* **155**, 307–315.

Zheng, L., Du, Z., Lin, C., Mao, Q., Wu, K., Wu, J., Wei, T., Wu, Z. and Xie, L. (2015) *Rice stripe tenuivirus* p2 may recruit or manipulate nucleolar functions through an interaction with fibrillarin to promote virus systemic movement. *Mol. Plant Pathol.* **16**, 921–930.

SUPPORTING INFORMATION

Additional supporting information may be found in the online version of this article at the publisher's web-site:

Fig. S1 Involvement of the importin α/β pathway for Triple Gene Block1 (TGB1) transport to the nucleus. (A) Bimolecular fluorescence complementation (BiFC) identification of interactions between TGB1 and Impα. Reconstitution of yellow fluorescent protein (YFP) fluorescence in the nucleus during co-expression of TGB1-nYFP with Impα-cYFP, or TGB1-cYFP with Impα-nYFP, in *Nicotiana benthamiana* epidermal cells. Bars, 20 μm. (B) Glutathione *S*-transferase (GST) affinity assays of interactions between TGB1 and Impα. TGB1 was pulled down by GST-Impα (Lane 1), but not by GST-GFP (Lane 2), and GFP-His was not pulled down by GST-Impα (Lane 3). GFP, green fluorescent protein.

Fig. S2 Subcellular localization of Triple Gene Block1 (TGB1) fused with a nuclear localization signal (NLS) (row 2) and its non-functional mutant nls (row 3), nuclear export signal (NES)

(row 4) and its non-functional nes mutant (row 5). Fibrillarin-red fluorescent protein (Fib2-RFP) was used as a nucleolar marker. Leaves were observed at 3 days post-infiltration (dpi). See Fig. 1C for depiction of the *Barley stripe mosaic virus* (BSMV) derivatives. GFP, green fluorescent protein. Bars, 5 μm.

Fig. S3 Reverse transcription-polymerase chain reaction (RT-PCR) detection of *Barley stripe mosaic virus* (BSMV) in the upper leaves. (A) Detection of BSMV RNA in BSMV, BSMV NLS-TGB1, nls-TGB1, NES-TGB1 and nes-TGB1 BSMV derivatives in the upper leaves of agroinfiltrated *Nicotiana benthamiana* plants. See Fig. 1C for depiction of the BSMV derivatives. (B) Detection of BSMV RNA in the upper leaves of *N. benthamiana* agroinfiltrated with BSMV, or combinations of the TGB1 nucleolar and nuclear mutant viruses. See Fig. 4A for depiction of the $BSMV_{mNoLS}$, $BSMV_{mNLS}$ and $BSMV_{mNoLS/mNLS}$ mutants. Leaf samples were collected at 14 days post-infiltration (dpi) for RT-PCR analyses of the 5′-untranslated region (5′-UTR) of the γ strand.

Fig. S4 Confocal microscopy showing the subcellular localization of the Triple Gene Block1 (TGB1) site-specific N_{240}-GFP, N_{240}Am-GFP, N_{240}Bm-GFP, N_{240}ABm-GFP and C_{272}-GFP. Plasmids encoding the mutant proteins were agroinfiltrated into *Nicotiana benthamiana* leaves, and the infiltrated leaves were taken and subjected to confocal microscopy examination at 3 days post-infiltration (dpi). GFP, green fluorescent protein; RFP, red fluorescent protein. Bars, 20 μm.

Fig. S5 Western blot and reverse transcription-polymerase chain reaction (RT-PCR) detection of *Barley stripe mosaic virus* (BSMV) in barley. Symptoms of emerging barley leaves at 14 days post-infiltration (dpi) with *in vitro* transcripts of BSMV, or the nucleolar and nuclear mutation viruses. Plants were inoculated at the two-leaf stage of development. Samples of the upper leaves were collected at 14 dpi for western blot analyses for detection of the coat protein (CP) and the Triple Gene Block1 (TGB1) protein, and RT-PCR to detect viral RNA. Ribulose-1,5-bisphosphate carboxylase/oxygenase (Rubisco) indicates equal sample loading.

Fig. S6 Generation of RNAi-*fib2* transgenic plants. (A) Schematic depiction of the RNAi-*fib2* hairpin plasmid, pMDC32. LB, left border; RB, right border. (B) Top panel: symptoms of non-transgenic (NT) *Nicotiana benthamiana* plants, and the 2d and 6a RNAi-*fib2* transgenic lines. Middle panel: polymerase chain reaction (PCR) detection of the screening marker gene *hygromycin* in transformed plants. Bottom panel: detection of fibrillarin (Fib2) protein in the NT, 2d and 6a lines. CK+, positive PCR control; M, protein markers; NT, non-transgenic; Rubisco, ribulose-1,5-bisphosphate carboxylase/oxygenase.

Fig. S7 Confocal microscopy showing the co-expression of green fluorescent protein (GFP) and red fluorescent protein-fibrillarin (RFP-Fib2) in *Nicotiana benthamiana* leaf cells at 3 days after agroinfiltration with *Agrobacterium* strains harbouring the plasmids. Bars, 20 μm.

Fig. S8 Alignments of the Triple Gene Block1 (TGB1) proteins amongst nine sequenced *Barley stripe mosaic virus* (BSMV) strains. The GenBank accession numbers of the TGB1 proteins are AAA79153.1 (ND18), AAA79161.1 (Type), AIT18337.1 (Xinjiang), AAA79149.1 (CV17), AAA79157.1 (CV42), AHY22369.1 (Qasr Ibrim, QI), AEP04415.1 (Norwich), AAV67981.1 (Beijing) and NP_604487.1 (Type ATCC-PV43, PV43). NoLS, nucleolar localization signal.

Fig. S9 Alignments of the *Barley stripe mosaic virus* (BSMV), *Poa semilatent virus* (PSLV) and *Lychnis ringspot virus* (LRSV) hordeivirus Triple Gene Block1 (TGB1) proteins. The GenBank accession numbers of the TGB1 proteins are AAA79153.1 (BSMV-TGB1), AAB05577.1 (PSLV-TGB1) and CAA86470.1 (LRSV-TGB1). The underscored sequences show the PSLV NoLS sequences. NLS, nuclear localization signal. NoLS, nucleolar localization signal.

Table S1 Primers used in this study.

Table S2 Systemic infectivity of *Nicotiana benthamiana* by *Barley stripe mosaic virus* (BSMV) and the NLS/nls or NES/nes insertion derivatives at the Triple Gene Block1 (TGB1) N-terminus of the BSMV mutants.

Table S3 Systemic infectivity of the *Barley stripe mosaic virus* (BSMV) NoLS- or NLS-related mutants in *Nicotiana benthamiana* and barley.

Text S1 Supporting experimental procedures.